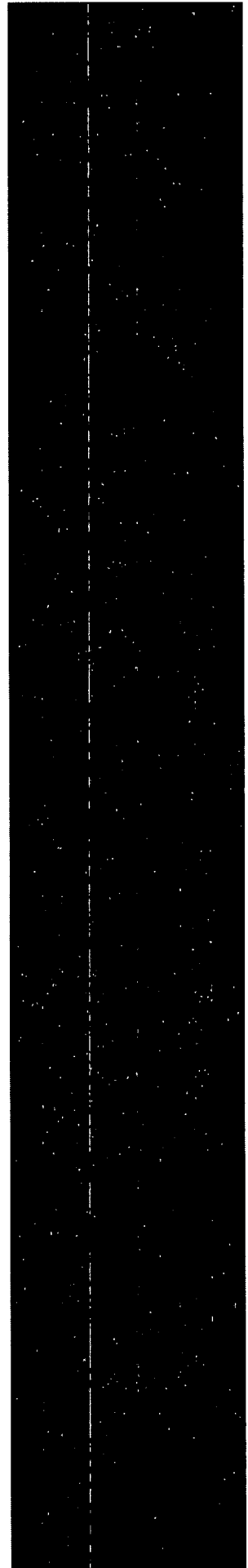


**Atmospheric Stress Corrosion
Cracking Susceptibility of Welded and
Unwelded 304, 304L, and 316L
Austenitic Stainless Steels
Commonly Used for Dry Cask
Storage Containers Exposed to
Marine Environments**



AVAILABILITY OF REFERENCE MATERIALS IN NRC PUBLICATIONS

NRC Reference Material

As of November 1999, you may electronically access NUREG-series publications and other NRC records at NRC's Public Electronic Reading Room at <http://www.nrc.gov/reading-rm.html>. Publicly released records include, to name a few, NUREG-series publications; *Federal Register* notices; applicant, licensee, and vendor documents and correspondence; NRC correspondence and internal memoranda; bulletins and information notices; inspection and investigative reports; licensee event reports; and Commission papers and their attachments.

NRC publications in the NUREG series, NRC regulations, and *Title 10, Energy*, in the Code of *Federal Regulations* may also be purchased from one of these two sources.

1. The Superintendent of Documents
U.S. Government Printing Office
Mail Stop SSOP
Washington, DC 20402-0001
Internet: bookstore.gpo.gov
Telephone: 202-512-1800
Fax: 202-512-2250
2. The National Technical Information Service
Springfield, VA 22161-0002
www.ntis.gov
1-800-553-6847 or, locally, 703-605-6000

A single copy of each NRC draft report for comment is available free, to the extent of supply, upon written request as follows:

Address: U.S. Nuclear Regulatory Commission
Office of Administration
Mail, Distribution and Messenger Team
Washington, DC 20555-0001

E-mail: DISTRIBUTION@nrc.gov
Facsimile: 301-415-2289

Some publications in the NUREG series that are posted at NRC's Web site address <http://www.nrc.gov/reading-rm/doc-collections/nuregs> are updated periodically and may differ from the last printed version. Although references to material found on a Web site bear the date the material was accessed, the material available on the date cited may subsequently be removed from the site.

Non-NRC Reference Material

Documents available from public and special technical libraries include all open literature items, such as books, journal articles, and transactions, *Federal Register* notices, Federal and State legislation, and congressional reports. Such documents as theses, dissertations, foreign reports and translations, and non-NRC conference proceedings may be purchased from their sponsoring organization.

Copies of industry codes and standards used in a substantive manner in the NRC regulatory process are maintained at—

The NRC Technical Library
Two White Flint North
11545 Rockville Pike
Rockville, MD 20852-2738

These standards are available in the library for reference use by the public. Codes and standards are usually copyrighted and may be purchased from the originating organization or, if they are American National Standards, from—

American National Standards Institute
11 West 42nd Street
New York, NY 10036-8002
www.ansi.org
212-642-4900

Legally binding regulatory requirements are stated only in laws; NRC regulations; licenses, including technical specifications; or orders, not in NUREG-series publications. The views expressed in contractor-prepared publications in this series are not necessarily those of the NRC.

The NUREG series comprises (1) technical and administrative reports and books prepared by the staff (NUREG-XXXX) or agency contractors (NUREG/CR-XXXX), (2) proceedings of conferences (NUREG/CP-XXXX), (3) reports resulting from international agreements (NUREG/IA-XXXX), (4) brochures (NUREG/BR-XXXX), and (5) compilations of legal decisions and orders of the Commission and Atomic and Safety Licensing Boards and of Directors' decisions under Section 2.206 of NRC's regulations (NUREG-0750).

DISCLAIMER: This report was prepared as an account of work sponsored by an agency of the U.S. Government. Neither the U.S. Government nor any agency thereof, nor any employee, makes any warranty, expressed or implied, or assumes any legal liability or responsibility for any third party's use, or the results of such use, of any information, apparatus, product, or process disclosed in this publication, or represents that its use by such third party would not infringe privately owned rights.

**Atmospheric Stress Corrosion
Cracking Susceptibility of Welded and
Unwelded 304, 304L, and 316L
Austenitic Stainless Steels
Commonly Used for Dry Cask
Storage Containers Exposed to
Marine Environments**

Manuscript Completed: June 2010
Date Published: October 2010

Prepared by
L. Caseres and T.S. Mintz

Southwest Research Institute
6220 Culebra Road
San Antonio, TX 78228

M.M. Bayssie, NRC Project Manager

NRC Job Code N6195

Office of Nuclear Regulatory Research

ABSTRACT

This report documents information on the susceptibility to atmospheric stress corrosion cracking of welded and unwelded 304, 304L, and 316L austenitic stainless steels commonly used for dry storage containers exposed to marine environments. Standard U-bend specimens were exposed to both salt spray and salt fog conditions at temperatures ranging from 25 to 176 °C [77 to 350 °F] and varying relative humidity. The first test conducted was a salt spray test to scope out material and residual stress effects. This deliberately conservative test resulted in extensive cracking and corrosion as was observed in all the 93 and 176 °C [200 and 350 °F] U-bends in as early as 1 month after exposure. Salt spray tests are non-prototypical since deposition of salt on dry casks is in the form of a dry aerosol; hence, the first test was not suitable for evaluation of stress corrosion cracking susceptibility of austenitic stainless steels in coastal atmospheres. The second test conducted, the salt fog test, was expected to closely simulate field conditions around dry cask containers, and resulted in stress corrosion cracking and pitting corrosion in all the 43 °C [109 °F] specimens. Corrosion developed after 4 weeks in the 304 and 304L specimens, and after 32 weeks in the 316L specimen. This suggests that the alloy composition plays a role in stress corrosion cracking susceptibility. Cracking was mainly transgranular with sections of intergranular branching. Cracks were concentrated within the arch region in all unwelded U-bends and at the heat-affected zone of the welded specimens, as previously reported in the literature. None of the 85 and 120 °C [185 and 248 °F] specimens exposed to the salt fog test exhibited stress corrosion cracking; the data are consistent with the inability of salt deposits to deliquesce at high temperatures.

The tests indicate that chloride-induced stress corrosion cracking is highly dependent on the concentration of deposited sea salt, residual stress, cask temperature and the relative humidity of the surrounding environment. The results of the salt fog test may be conservative because the high absolute humidity used for the test was chosen to bound natural conditions expected in the dry storage cask environment. However, the results are still pertinent because they demonstrate that the deliquescence of dry deposited sea salt can lead to stress corrosion cracking of austenitic stainless steels at temperatures that are only slightly greater than ambient temperatures. The SCC acceleration factor used in laboratory testing and its implication on SCC initiation in actual dry storage cask units in the field are difficult to compute. Under the assumptions presented in this report, which simulate ideal conditions for the onset of SCC, initiation would be expected between 32 and 128 weeks. However, this is still a rough estimation because it does not take into account the operating history of the dry storage cask and the local environmental properties at each cask location.



FOREWORD

During refueling operations at domestic nuclear power plants, fuel that has been removed from the reactor is stored in spent fuel pools. Because the available space in the spent fuel pools of many commercial nuclear power plants has reached capacity some plants are currently, or planning to store spent fuel in NRC-licensed dry storage systems. For plants located near coastal areas, chloride stress corrosion cracking (SCC) is a potential degradation mode for dry storage system canisters made from austenitic stainless steels. Previous research on chloride SCC of austenitic stainless steels provides some insight on the effects of material composition and condition; however, limited information is available to determine the susceptibility of dry storage system canisters placed inside a ventilated concrete enclosure.

In this research program, an accelerated test method was developed and used to evaluate factors that affect the chloride SCC of austenitic stainless steels. Testing was conducted using standardized test specimens with and without welds. The test specimens were placed in a test chamber, heated to simulate the range of expected canister surface temperatures, and exposed to conditions that simulate coastal environments. Test results indicate dry sea salt deposits exposed to environments with high relative humidity leads to the formation of chloride containing solutions necessary for chloride SCC of austenitic stainless steels. The SCC susceptibility is influenced by both temperature and alloy composition.

Although the accelerated test method employed may be conservative compared to typical field conditions, the results are relevant and indicate long-term operation and accumulation of sea salts may lead to conditions where chloride SCC of austenitic stainless steel canisters is possible. The results of this should be considered in the licensing and operation of dry cask storage installations in coastal environments.

/RA/

Michael Case, Director
Division of Engineering
Office of Nuclear Regulatory Research

CONTENTS

ABSTRACT.....	iii
FOREWORD	v
FIGURES.....	ix
TABLES	xiii
EXECUTIVE SUMMARY	xv
ACKNOWLEDGEMENTS	xvii
1 INTRODUCTION.....	1
1.1 Stress Corrosion Cracking Background	1
1.2 Objective	3
1.3 Scope of Work and Report Organization.....	3
2 EXPERIMENTAL PROCEDURE	5
2.1 Salt Spray and Salt Fog Tests.....	5
2.1.1 U-Bend Specimen Fabrication	5
2.1.2 Environmental Chambers	8
2.1.3 Salt Spray Testing Protocol	11
2.1.4 Salt Fog Testing Protocol.....	12
2.1.5 Examination of SCC.....	16
2.1.6 Salt Chemical Composition and Deposition Rates	17
2.2 SCC Complementary Testing.....	18
2.2.1 Environmental Temperature and Humidity Profiles	18
2.2.2 Salt Deliquescence and Efflorescence	18
2.2.3 Controlled Relative Humidity/Temperature Tests	19
3 SALT SPRAY TESTING RESULTS.....	21
3.1 U-Bend Specimens Held At 25 °C [77 °F]	21
3.2 U-Bend Specimens Held At 93 °C [200 °F]	21
3.3 U-Bend Specimens Held At 176 °C [350 °F]	23
3.4 Discussion	25
4 SALT FOG TESTING RESULTS	29
4.1 U-Bend Specimens Held At 43 °C [109 °F]	30
4.1.1 Results of the 4-Week Exposure Time	30
4.1.2 Results of the 16-Week Exposure Time	31
4.1.3 Results of the 32-Week Exposure Time	33
4.1.4 Results of the 52-Week Exposure Time	38
4.2 U-Bend Specimens Held At 85 °C [185 °F] and 120 °C [248 °F]	38
4.3 Salt Chemical Composition and Deposition Rates	40
4.4 Discussion	44
4.5 Implications of the Results	48
5 SCC COMPLIMENTARY TESTING.....	51
5.1 Half U-Bend Specimen Testing	51
5.2 Salt Deliquescence and Efflorescence	54
5.3 Environmental Temperature and Humidity Profiles	56
5.4 Discussion	57

CONTENTS (CONTINUED)

6	CONCLUSIONS.....	59
7	RECOMMENDATIONS.....	61
8	REFERENCES.....	63

FIGURES

Figure		Page
1	U-Bend Specimen Fabrication with Respect to the Sheet Rolling Direction (Specimen Dimensions not to Scale).....	7
2	Configuration of the Single and Double U-Bend Specimens	7
3	Picture of the Standardized Auto Technology Environmental Chamber	9
4	Picture of the Custom Stainless Steel Environmental Chamber	9
5	U-Bend Specimens Placed on Cartridge Heaters in the Custom Environmental Chamber	10
6	PID Controllers Used to Set and Control the Temperature of the Cartridge Heaters.....	10
7	Schematics of the Locations of Thermocouples Attached to Selected Single and Double U-Bend Specimens for Temperature Profile Determination.....	12
8	Typical Appearance of the Half U-Bend Samples Used for Salt Deposition Measurements After 2 Weeks of Exposure.....	15
9	Schematic of the U-Bend Specimen Arrangement on Each Cartridge Heater.....	15
10	(a) Schematic of the Cartridge Heater Layout and (b) a Picture of the Standardized Atmospheric Chamber	16
11	Typical U-Bend Arrangement Used for the Salt Spray and Salt Fog Tests.....	16
12	Photograph of the Flat Specimens Exposed to 85 °C [185 °F] Used for the Salt Deposition Rate Determination. The Specimens Appeared to be Completely White Because of the Deposited Salt.....	17
13	Typical Surface Appearance of the Single U-Bend Specimens: (a) 304, (b) 304L, and (c) 316L Held at 25 °C [77 °F] for a 1-Month Exposure	21
14	Typical SCC Behavior of the 304 Stainless Steel (a) Single and (b) Double U-Bend Specimens Exposed for 1 Month at a Temperature of 93 °C [200 °F]	22
15	Typical SCC Behavior of a 304L Stainless Steel Single U-Bend Specimen Exposed for 1 Month at a Temperature of 93 °C [200 °F].....	23
16	Typical SCC Behavior of a 316L Stainless Steel Single U-Bend Specimen Exposed for 1 Month at a Temperature of 93 °C [200 °F].....	23
17	Typical SCC Behavior of a 304 Stainless Steel Single U-Bend Specimen Exposed for 1 Month at a Temperature of 176 °C [350 °F].....	24
18	Typical SCC Behavior of a 304 Stainless Steel Double U-Bend Specimen Exposed for 1 Month at a Temperature of 176 °C [350 °F].....	25
19	Typical SCC Behavior of the Inner 316L Stainless Steel Double U-Bend Specimen Exposed for 1 Month at a Temperature of 176 °C [350 °F].....	25
20	Temperature Profile for a) Single and (b) Double U-Bend Specimens at 93 °C [200 °F] Subjected to the Salt Spray Test.....	27
21	Temperature Profile for (a) Single and (b) Double U-Bend Specimens at 176 °C [350 °F] Subjected to the Salt Spray Test.....	28

FIGURES

Figure		Page
22	Chamber Temperature, Relative Humidity, and Absolute Humidity Trends as a Function of Time for Two Consecutive Full Cycles Recorded During the Salt Fog Test	30
23	Pictures of Selected 43 °C [109 °F] 304 and 304L Weld U-Bend Specimens and an Overall Photograph of all the 43 °C [109 °F] Specimens Mounted on the Heaters 16, 17, and 18 in the Environmental Chamber after 4 Weeks of Exposure. The Specimen Arrangement in Each Heater is Shown in Figure 9	31
24	Pictures of (a) a 43 °C [109 °F] 304L U-Bend Specimen Showing Corrosion Product and Striation Marks on the Surface, (b) Corrosion Distress of the 304 Weld U-Bend Specimens, and (c) a 304 Double U-Bend Specimen After 16 Weeks of Exposure	32
25	Pictures of SCC Observed Near the Outer Surface at the Specimen Arch: (a and b) a 304 Single U-Bend Specimen and (c and d) a 304L Single U-Bend Specimen. Both Samples Were Exposed to 43 °C [109 °F] for 16 Weeks of Exposure	33
26	Pictures of a Cleaned 304 Stainless Steel U-Bend Specimen Exposed for 32 Weeks at a Temperature of 43 °C [109 °F]	34
27	Pictures of a Cleaned 304L Stainless Steel U-Bend Specimen Exposed for 32 Weeks at a Temperature of 43 °C [109 °F]	34
28	Stereomicroscopic Images of a 316L Stainless Steel: (a) Single, and b) Welded U-Bend Specimens	35
29	Pictures of Cut Stainless Steel U-Bend Specimens for Microstructure Evaluation	35
30	Stereomicroscopic Image of the Cut 304L Weld U-Bend	36
31	Stereomicroscopic Image of a Cleaned 316L Weld U-Bend Exposed for 32 Weeks at a Temperature of 43 °C [109 °F]	36
32	Stereomicroscopic Image of a Cleaned 304L Weld U-Bend Exposed for 32 Weeks at a Temperature of 43 °C [109 °F]	37
33	Stereomicroscopic Image of a Cleaned 304 Unwelded Single U-Bend Exposed for 32 Weeks at a Temperature of 43 °C [109 °F]	37
34	Typical Surface Appearances of Unwelded Single U-Bend Specimens Exposed for 52 Weeks at 43 °C [109 °F]. Striation Marks on the Outer Surface of the 304 and 304L Unwelded Specimens are Indicated	38
35	Pictures of the U-Bend Specimens Exposed to (a) 120 °C [248 °F] and (b) 85 °C [185 °F] for 52 Weeks of Exposure	39
36	Pictures of the U-Bend Specimens Exposed to (a) 120 °C [248 °F] and (b) 85 °C [185 °F] for 4 Weeks	39
37	Pictures of the U-Bend Specimens (a) 120 °C [248 °F] and (b) 85 °C [185 °F] Before Removal from the Environmental Chamber After 52 Weeks	40

FIGURES

Figure	Page
38	Optical Examinations of the Weld/Heat-Affected Zone of (a) a 304 U-Bend Specimen and (b) a 316L U-Bend Specimen. Both Specimens Were Exposed to 85 °C [185 °F] for 32 Weeks 40
39	Salt Deposition Rates as a Function of Time for the Half U-Bend Samples Exposed to Salt Fog. Due to the Condensation Issue Inside the Chamber, the Salt Deposition Rates for the 120 °C [248 °F] Samples are Inaccurate Between 100 and 365 Days of Exposure 43
40	SCC Susceptibility Map for the Type 304 Stainless Steel (Number in Parenthesis States Number of Specimens Cracked/Total Number of Specimens Tested) 44
41	SCC Susceptibility Map for the Type 304L Stainless Steel (Number in Parenthesis States Number of Specimens Cracked/Total Number of Specimens Tested) 45
42	SCC Susceptibility Map for the Type 316L Stainless Steel (Number in Parenthesis States Number of Specimens Cracked/Total Number of Specimens Tested) 45
43	Evolution of the Relative Humidity as a Function of Temperature Computed for Various Absolute Humidity Values. The Region Between the Red (Maximum Humidity) and Blue (Minimum Humidity) Symbols Indicate the Expected Environmental Conditions Near the U-Bend Surface in the Salt Fog Test..... 48
44	Typical Surface Appearance Observed for the 304 Stainless Steel Half U-Bend Samples Subjected to 2-Month at 65 °C [149 °F] and 70 Percent Relative Humidity 52
45	Laser Profilometer Data Evaluating Depth of Pitting on a 304 Stainless Steel Half U-Bend Sample Exposed to 2-Month at 65 °C [149 °F] and 70 Percent Relative Humidity 52
46	Typical Surface Appearance (Before Cleaning) of the 304 Stainless Steel Half U-Bends Exposed to 50 °C [122 °F] and 65 Percent Relative Humidity for 2 Months:(a) Initial Salt Deposits on the Surface During the Salt Fog Test, (b) Simulated Sea Salt Droplets, (c) Sodium Chloride Droplets, and (d) Magnesium Chloride Droplets 53
47	Typical Surface Appearance (Before Cleaning) of the 304 Stainless Steel Half U-Bends Exposed to 50 °C [122 °F] and 40 Percent Relative Humidity for 2 Months:(a) Initial Salt Deposits on the Surface During the Salt Fog Test, (b) Simulated Sea Salt Droplets, (c) Sodium Chloride Droplets, and (d) Magnesium Chloride Droplets 53
48	Typical Surface Appearance (Before Cleaning) of the 304 Stainless Steel Half U-Bends Exposed to 50 °C [122 °F] and 50 Percent Relative Humidity for 2 Months:(a) Initial Salt Deposits on the Surface During the Salt Fog Test, (b) Simulated Sea Salt Droplets, (c) Sodium Chloride Droplets, and (d) Magnesium Chloride Droplets 53

FIGURES

Figure		Page
49	Deliquescence Experiments Conducted at 50 °C [122 °F] and Relative Humidity of (a) 20 Percent, (b) 35 Percent, (c) 45 Percent, (d) 55 Percent, (e) 65 Percent, and (f) 75 Percent. The Salt Sample Labels are (A) Corpus Christi Salt, (B) Simulated Sea Salt, (C) Sodium Chloride, and (D) Magnesium Chloride	55
50	Temperature, Absolute Humidity, and Relative Humidity Profiles as a Function of Distance from the U-Bend Samples Heated at Different Temperatures	56

TABLES

Table	Page
1	Composition of the Stainless Steel Alloys and the Filler Materials Used for Welding 6
2	Modified GM 9540P Accelerated Test Procedure for the Salt Spray Testing 11
3	Accelerated Corrosion Cycles of the Salt Fog Test 14
4	Temperature and Relative Humidity Parameters Controlled Relative Humidity/Temperature Tests 19
5	Chemical Analyses of a Salt Portion Collected from the Surface of Selected 85 °C [185 °F] U-Bend Specimens 41
6	Chemical Analyses of a Salt Portion Collected from the Surface of Selected 120 °C [248 °F] U-Bend Specimens 41
7	Ratio of Anion Concentration to Chloride Concentration of the Deposited Salt and the Bulk ASTM Sea Salt 41
8	Ratio of Cation Concentration to Sodium Concentration of the Deposited Salt and the Bulk ASTM Sea Salt 42
9	Salt Deposit Results for the Flat Specimens After a 2-Week Exposure 42
10	Salt Deposit Results for the Half U-Bend Samples During the Salt Fog Test 43

EXECUTIVE SUMMARY

Currently, 60 of the 104 operating nuclear power plants have onsite dry storage systems for spent nuclear fuel. These dry storage systems, which consist of an austenitic stainless steel canister housed inside either an outer storage cask or a concrete vault, are necessary because of the limited room available in spent fuel storage pools. Some of these dry storage systems are located in chloride-rich environments near coastal areas, which may lead to deposition of chloride salts on the canister surface. Because many of the dry storage canisters are made of austenitic stainless steels, a potential concern is the susceptibility of these alloys to chloride-induced stress corrosion cracking (SCC). While much of the research on chloride-induced SCC of austenitic stainless steel gives insight about the degradation mechanisms and material performance, there is limited information on SCC in the range of environmental conditions associated with spent fuel dry storage canisters placed inside a ventilated outer storage cask or a concrete vault.

To address the above issue, the SCC susceptibility of austenitic stainless steels used in exposed to humid chloride-rich environments was investigated, using both salt spray and salt fog tests. Materials studied included types 304, 304L, and 316L stainless steel alloys with and without welds. The alloys were bent in a U-shape according to the ASTM G30 standard procedure to generate internal tensile stresses, mounted on cartridge heaters, and placed inside an atmospheric chamber. The SCC susceptibility was evaluated as a function of the alloy composition and specimen temperature.

The salt spray test consisted of cyclically spraying the specimen surface with simulated sea salt solution, following the guidelines an industrial standard for accelerated corrosion testing. SCC susceptibility was evaluated using single and double unwelded U-bend specimens maintained at three different temperatures: 25, 93, and 176 °C [77, 200, and 350 °F]. The results of this test showed no cracking events for all the 25 °C [77 °F] specimens, whereas extensive cracking was observed for all the 93 °C [200 °F] and 176 °C [350 °F] U-bends after 1 month of exposure. Cracking on specimens tested at 176 °C [350 °F] was noted on areas of the specimens that were not in contact with the cartridge heaters. These areas of the specimens were not maintained at the desired test temperature. In addition, these areas of the U-bend specimens were cooled below boiling for brief periods after the short salt water spray cycles. Results of the initial tests indicated that spraying simulated seawater on the test materials was not an appropriate accelerated test method for evaluating atmospheric SCC susceptibility.

Consequently, a salt fog test was developed to more closely simulate dry storage cask field conditions. This test consisted of phases to deposit simulated sea salt on the surface of the U-bend and exposure of the specimens to controlled high and low relative humidity conditions. U-bend specimens were tested in triplicate for 4, 16, 32, and 52 weeks of exposure at 43, 85, and 120 °C [109, 185, and 248 °F].

The results of this test showed that all the 304 and 304L specimens maintained at 43 °C [109 °F] exhibited cracking as well as significant corrosion distress in as early as 4 weeks after exposure. Cracking of the 43 °C [109 °F] 316L stainless steel specimens occurred after 32 weeks of exposure. This suggests, as expected, that the alloy composition plays a role in the SCC susceptibility. Both isolated corrosion pits and general corrosion were observed on all of the 43 °C [109 °F] specimens. Cracking was concentrated within the arch area in all unwelded U-bends, where the tensile stresses were greatest, and at the heat-affected zone of the welded specimens. Microscopic evidence suggested that the cracks were mainly transgranular with sections of intergranular branching morphology. The extent of cracking and corrosion damage became more conspicuous as time progressed in all the alloys at this temperature. For a given alloy type, welded and unwelded U-bends showed comparable SCC susceptibility. On the other hand, none of the U-bend specimens at 85 and 120 °C [185 and 248 °F] exhibited SCC susceptibility, consistent with the inability of the salt to deliquesce, even during the high relative humidity cycles. Nevertheless, a few isolated shallow pits within the arch area were observed for all the welded alloys held at 85 °C [185 °F] after 4 months of exposure. No pits were observed in either the unwelded 85 °C [185 °F] specimens or the welded and unwelded 120 °C [248 °F] specimens.

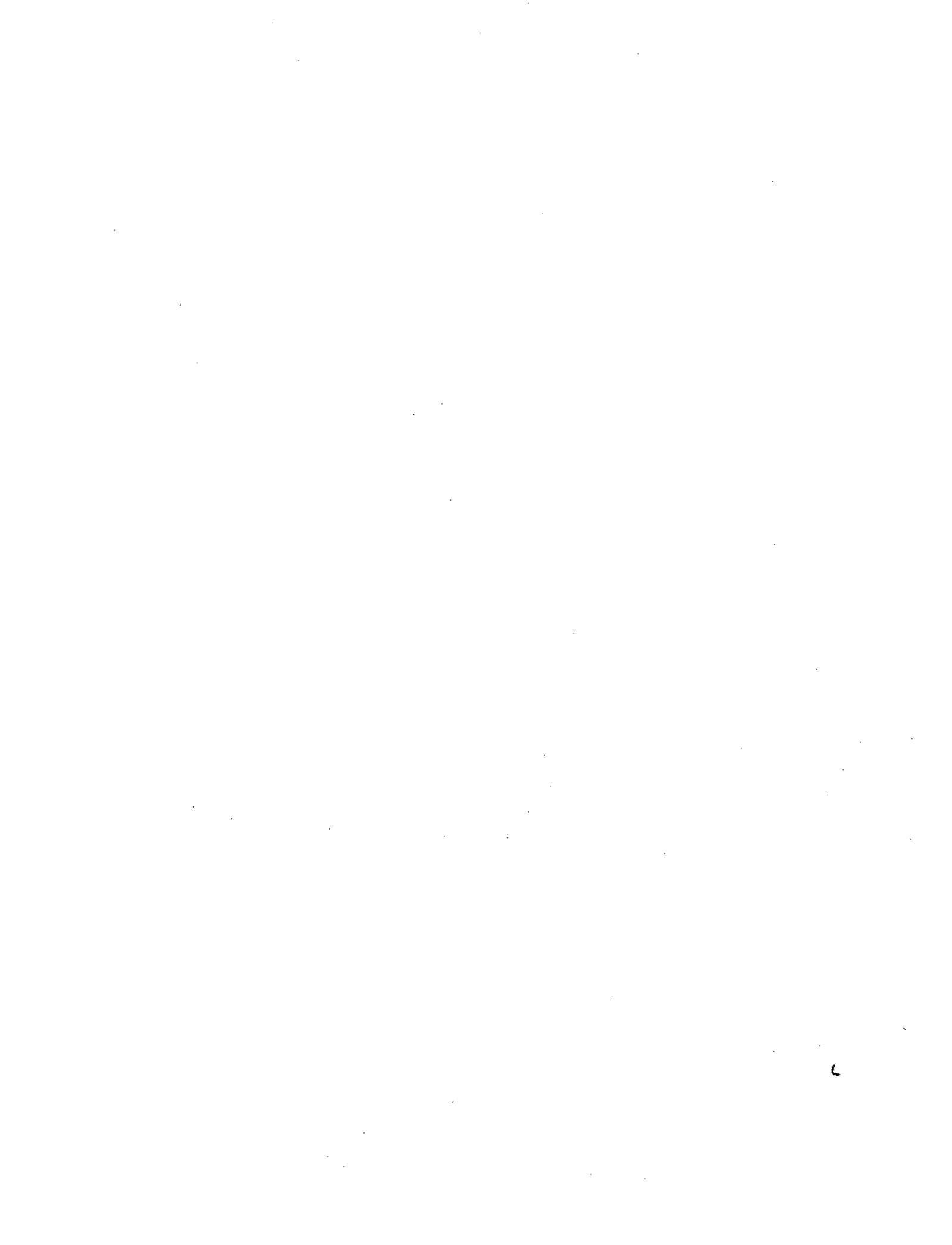
The dominant pit initiation, crack formation and propagation mechanisms are unclear based on the information obtained from this study. Literature information suggests that pit nucleation in unwelded stainless steels exposed to chloride containing solutions occurs mainly at or near manganese, sulfide and mixed oxide/sulfide inclusions present at the stainless steel surface. The dominant pit nucleation mechanisms are attributed to the local decrease in pH resulting from inclusion dissolution and chromium depletion surrounding the inclusions. Cracks started at or near the pits within the specimen arch and propagated through the specimen cross section. For welded stainless steels, the most common and relevant factors affecting pit initiation are related to the interdendritic attack in weld metal zone and sensitized grain boundaries in the heat-affected zone, resulting in localized chromium depletion.

Overall, the results obtained from this investigation indicate that chloride-induced SCC is highly dependent on the temperature of the cask surface and relative humidity of the surrounding environment. The observed salt fog test results are likely conservative because the high absolute humidity required for cracking may not be consistent with the actual conditions in a dry storage cask placed inside a concrete vault. However, the results demonstrate that deliquescence of dry deposited sea salt can lead to stress corrosion cracking of 304, 304L, and 316L stainless steel at slightly elevated temperatures. Based on the results of this investigation, estimation of the SCC acceleration factor used in the laboratory testing and its implications on durability and SCC development to actual dry storage cask units in the field are difficult to compute and requires various assumptions to be made. Under all the assumptions presented in this report, then, the time to SCC initiation would be expected to be roughly between 32 and 128 weeks. However, this is still a rough estimation because it does not take into account the operating history of the dry storage cask and the local environmental properties at each cask location.

ACKNOWLEDGMENTS

The authors greatly acknowledge the contributions made by Mr. B. Derby in setting up, conducting the environmental tests, microstructure evaluations as well as providing technical support. Mr. D. Noll and Mr. S. Clay helped in the preparation of the U-bends and test monitoring. Researchers from the Chemical and Engineering Division at Southwest Research Institute were responsible for the salt chemical analyses in this program. The authors wish to acknowledge the valuable contributions of Mr. D. Dunn in the early phase of this program. The authors are grateful to Dr. Robert Tregoning, Mr. Geoffrey Hornseth, and Dr. Mekonen Bayssie for many helpful discussions and reviews. Thanks to Mr. James Dante for the technical review.

This report describes work done by the Southwest Research Institute for the U.S. Nuclear Regulatory Commission (NRC) under Contract No. NRC-04-07-108. The activities reported here were carried out on behalf of the U.S. NRC, Office of Nuclear Regulatory Research. This report is an independent product of the Southwest Research Institute and does not necessarily reflect the views or regulatory position of the U.S. NRC.



1 INTRODUCTION

1.1 Stress Corrosion Cracking Background

The current fleet of nuclear reactors in the United States has been in operation for multiple decades. During the routine operation of nuclear power plants, spent fuel is removed from the reactor during outages and stored in spent fuel pools. However, because of the age of some of these nuclear power facilities and the amount of spent fuel produced, the spent fuel pools have reached capacity. As a result, nuclear power plants have been using NRC-licensed independent spent fuel storage installation (ISFSI), where spent fuel is contained in dry storage systems. Most of the dry storage systems use canisters that are made of austenitic stainless steel, including UNS S30400 (304 stainless steel), UNS S30403 (304L stainless steel), and UNS S31603 (316L stainless steel) (USNRC, 2003a; USNRC 2003b). The stainless steel canisters are placed either horizontally in concrete vaults or vertically inside steel and concrete outer casks that provide radiation shielding. The vertical outer storage casks and the concrete vaults are designed with air passages for passive air circulation so that the environment surrounding the cask interacts with outside air. As a result of their design, the outer storage cask and the concrete vaults prohibit precipitation from contacting the stainless steel canisters. Therefore, it is possible for airborne salts to reach the stainless steel canisters and accumulate on the surface over time. While there have been no reported cracking events within dry storage systems, it is well known that austenitic stainless steels are susceptible to chloride-induced stress corrosion cracking (SCC) in marine environments. Effectively, chloride-induced SCC can occur if three pre-conditions are met: a susceptible alloy or microstructure, sufficient applied or residual tensile stress, and a corrosive environment (Toshima and Ikeno, 2000; Huizinga et al., 2005; NASA, 1971, Wilde, 1971; Speidel, 1981; Cragnolino et al., 2001).

Alloy composition is a key factor in determining SCC susceptibility. Two chemical constituents known to influence SCC susceptibility of stainless steels are carbon and molybdenum. When raised to a temperature range between 400 and 800 °C [752 and 1472 °F], carbon diffuses towards the grain boundary and reacts with available chromium, forming chromium-rich carbides of a typical composition $\text{Cr}_{16}\text{Fe}_7\text{C}_6$ (Solomon, 1978; Szklarska-Smialowska et al., 1992). This process, known as sensitization, causes a depletion of chromium at the grain boundary, and thus, a decrease in the alloy corrosion resistance. It has been observed that 304 stainless steels become susceptible to intergranular SCC when the chromium concentration at the grain boundary is below 12 weight percent. As such, the nuclear industry has started using low carbon austenitic stainless steels (e.g., 316L or 304L), which have shown lower SCC susceptibility than the 304 alloy because of the reduced formation of chromium carbides. On the other hand, the addition of 2 to 3 percent molybdenum to the 316L stainless steels enhances the stability of the passive oxide layer, increasing its resistance to SCC (Hayes, et al., 2006; Macdonald, 1992; Leinonen, 1996; Tsuruta and Okamoto, 1992).

A second key factor associated with SCC is the level of the applied or residual stress present on a SCC susceptible alloy. The applied or residual stress must be sufficient for the initiation and

propagation of SCC. Assis and coworkers (2002) have shown that a typical welding process on a stainless steel canister can lead to residual stresses near the yield strength of the material. These high residual stresses are known to be sufficient to initiate SCC.

The final requirement for SCC to occur is related to the environmental conditions surrounding a stressed SCC susceptible alloy. In particular, the presence of chlorides in high humidity environments significantly increases the probability of SCC. As expected, the highest chloride levels (in the form of sodium, calcium, and magnesium chlorides) occur along the coast of the Atlantic and Pacific Oceans and the Gulf of Mexico. The metal corrosion rate is directly related to the chloride content in the atmosphere. The concentration of chlorides in the environment is dependent on the distance from a large body of salt water, altitude above sea level, and prevailing winds (Gustafsson and Franzén, 1996; Meira et al., 2006). The effect of sheltering on a metal corrosion and SCC resistance also plays an important role. Chlorides that accumulate on an exposed surface can be washed away by precipitation. It has been demonstrated that, for some materials, sheltered exposures facilitate higher corrosion rates than unsheltered exposures in marine environments (Larrabee, 1953).

The effect of SCC on austenitic stainless steel immersed in chloride-contaminated solutions has been extensively studied (Truman, 1977; Goldberg, 1976). It has been demonstrated that for decreasing chloride concentration, the SCC susceptibility of austenitic 304 stainless steel decreases. Goldberg (1976) reported a decreased time to cracking as the chloride concentration increased.

In addition to the environmental parameters and alloy composition, temperature is also a key parameter known to affect SCC susceptibility of stainless steels. The study by Goldberg (1976) showed that SCC of 316L stainless steels was unlikely in concentrated chloride solutions at a pH of 2 below 65 °C [149 °F]. Later, studies by Ford and Silverman (1980) on sensitized 304 stainless steels indicated that SCC was observed at temperatures as low as 40 °C [104 °F] if oxygen is available in significant amounts.

While there is ample research studies carried out on SCC of austenitic stainless steel in chloride solutions, there is limited information on SCC of austenitic stainless steels exposed to atmospheric environments that are comparable to those found in dry storage systems. A recent investigation by Prosek et al. (2009) found that cracking is possible for 304 and 316L stainless steels exposed to solution droplets of magnesium, sodium, or calcium chloride at temperatures as low as 30 °C [86 °F] and low relative humidity. By depositing 20 to 100 mg/m² [4.55 10⁻⁷ to 2.27 10⁻⁶ oz/in²] of chloride on the surface of 304 stainless steels, Fairweather et al. (2008) observed cracking at a temperature as low as 30 °C [86 °F] with an increased cracking frequency as the temperature was increased to 60 °C [140 °F]. Initiation and propagation of SCC of stainless steel storage casks were recently investigated by Tani et al. (2009) using welded 304L and 316L stainless steels were sprayed with seawater with a chloride surface coverage of 10 g/m² [2.28 10⁻⁴ oz/in²]. Under these conditions, Tani et al. (2009) determined that 304L stainless steels were susceptible to chloride SCC above 40 °C [104 °F]. Based on

the literature data, it appears that cracking is more difficult to initiate at low temperatures, although the threshold temperature for SCC of stainless steels is dependent upon the environmental conditions, salt composition, and chloride concentration.

Both salt deliquescence and efflorescence play a role in SCC susceptibility of stainless steel exposed to marine environments. By definition, the process where salt absorbs moisture from the air to become a liquid is known as deliquescence. The opposite phenomenon, where the air pulls moisture out of a salt solution resulting in the formation of a solid salt is called efflorescence. The salt deliquescence and efflorescence occur at specific relative humidity values at a given temperature. Because of the kinetic effects, the deliquescence and efflorescence relative humidity values are not typically equal and the relative humidity where a salt undergoes efflorescence can be significantly lower than the relative humidity for salt deliquescence. Salts will deliquesce at various relative humidity depending upon chemistry and molecular size of the salts (Twomey, 1953; Owens, 1926; Winkler, 1988). The concentration and composition of atmospheric sea salts vary by geography. However, the typical constituents dictating the deliquescence and efflorescence points tend to be sodium and magnesium chlorides.

1.2 Objective

The objective of this research program was to evaluate the SCC susceptibility of welded and unwelded austenitic stainless steels that are commonly used in dry storage systems situated in humid, chloride-rich environments. Materials studied included the types 304, 304L, and 316L stainless steel alloys. The specimens from each alloy were bent in a U-shape to generate internal tensile stresses and mounted on cartridge heaters inside an atmospheric chamber. The SCC susceptibility was determined as a function of the alloy composition and specimen temperature using both salt spray and salt fog tests.

1.3 Scope of Work and Report Organization

The project was divided into two main tasks. The first task, described in Section 3 of this report, examined the SCC susceptibility of U-bend stainless steels using a direct salt spray test. This test can be considered an extremely conservative approach since dry storage casks are sheltered from the external environment by a concrete enclosure. The second task of this project, described in Section 4, examined the SCC susceptibility of U-bend stainless steels using a salt fog test. This test was intended to be less conservative than the direct salt spray test and more representative of dry storage systems sites located in coastal atmospheres with sea salt aerosols.

The outcome of the salt fog test led to complementary experiments, including salt deliquescence and efflorescence, atmospheric profile testing, and SCC testing in various controlled humidity/temperature environments. The salt deliquescence and efflorescence experiments were carried out to determine the conditions necessary for moisture absorption of

several salts at constant representative temperatures. The atmospheric profile testing was studied to measure the temperature and relative humidity profile around the heated specimens. Lastly, the SCC testing in controlled humidity/temperature environments was examined to support the evaluation of SCC initiation in these materials. Results of these complementary tests are presented in Section 5. Section 6 summarizes the findings of this research program and Section 7 provides recommendations for future technical research to diagnose SCC susceptibility of austenitic stainless steel canisters used in dry storage systems located in coastal atmospheres.

2 EXPERIMENTAL PROCEDURE

The experimental approach consisted of the implementation of three main types of tests: salt spray, salt fog, and complementary tests. The salt spray and salt fog tests were directly related to the evaluation of SCC susceptibility and are described in Section 2.1. The complementary tests were carried out in support of the salt fog test to determine SCC susceptibility under environmental conditions not explored in the other atmospheric tests.

2.1 Salt Spray and Salt Fog Tests

This section addresses the U-bend fabrication, instrumentation, and the experimental approaches used to determine the SCC behavior of austenitic stainless steels.

2.1.1 U-Bend Specimen Fabrication

Atmospheric SCC tests were carried out for 304, 304L, and 316L austenitic stainless steels with and without welds. The 304 and 304L welded specimens used 308 and 308L stainless steels as filler materials, respectively. The 316L stainless steel was welded with a 316L filler material. The chemical compositions of the alloys and the filler materials are shown in Table 1.

The alloys were purchased in sheet form with a nominal thickness of 0.318 cm [0.125 in]. The specimens to be bent were initially hydro-jet cut from the stock materials, so that the rolling direction¹ was perpendicular to the length of the specimens, as shown schematically in Figure 1. Through-thickness circular holes, 0.95 cm [0.375 in] diameter centered at 1.27 cm [0.5 in] from both specimen ends, were machined to accommodate an Alloy C-276 bolt and nut electrically isolated from the specimen by ceramic shoulder washers to maintain specimen displacement.

The U-bend specimens were fabricated by bending the flat specimens 180° around a 1.27 cm [0.5 in] diameter mandrill following the ASTM G30 standard procedure (ASTM, 1997). The U-bend specimens were kept in the mandrill under stress while the Alloy C-276 stressing elements were tightened to maintain specimen displacement. The strain $\epsilon = t/2R$ at the arch of the U-bend was estimated to be 0.25 in/in, where t is the specimen thickness and R is the radius of the bend.

Two types of specimens were prepared, single and double U-bend specimens. The latter was used to simulate a crevice environment. The single U-bend specimens were 12.7 cm [5 in] long and 1.9 cm [0.75 in] wide. The double U-bend specimens, made of 304 and 316L stainless

¹ SCC susceptibility is highly dependence on the specimen orientation as a function of the rolling direction. This test orientation was chosen because the expected resistance to SCC is lowest perpendicular to the rolling direction as cracking can propagate along the elongated grains in the rolling direction (ASM Handbooks, 2004).

steels², consisted of two overlapping specimens of the same alloy. The inner specimen had the same dimensions as the single U-bend, while the outer specimen was 13.65 cm [5.375 in] long and 1.9 cm [0.75 in] wide. Figure 2 shows the configuration of the single and double U-bend specimens without welds. Each U-bend specimen was inspected under a 50X magnification after bending to ensure that no cracks or fissures were present before testing.

In addition, half U-bend samples, 5.08 cm [2 in] long, 2.54 cm [1 in] wide and 0.317 cm [0.125 in] thick, were placed in the center of each cartridge heater during the salt fog test for salt deposition monitoring and temperature control as described in Section 2.1.6. Additional half U-bend samples were used for SCC evaluation in environments other than those studied in the atmospheric chambers as described in Section 2.2.3. The fabrication of the half U-bend samples was similar to the U-bends except that the half U-bends did not have extended legs or the stressing elements. This allowed for easy removal from the cartridge heaters.

Table 1 Composition of the Stainless Steel Alloys and the Filler Materials Used for Welding

Material	Fe	Cr	Ni	Mo	Mn	C	S	P	N	Si	Cu
Type 304	Bal	18.19	8.07	N/A	1.21	0.039	0.002	0.026	0.042	0.55	N/A
Type 304L	Bal	18.14	8.07	0.18	1.29	0.025	0.001	0.025	0.032	0.34	0.27
Type 316L	Bal	16.43	10.13	2.06	1.35	0.019	0.0006	0.027	0.022	0.51	0.32
ER308	Bal	19.92	9.61	0.10	1.35	0.051	0.002	0.023	0.019	0.36	0.14
ER308L	Bal	20.12	9.79	0.05	1.75	0.009	0.010	0.014	0.043	0.47	0.05
ER316L	Bal	18.10	11.05	2.22	1.63	0.023	0.016	0.026	0.04	0.41	0.39

Mill test reports supplied by Ta Chen International Co., AK Steel, and Inweld Co. For confirmation purposes, An-Tech Laboratories Inc. carried out mill tests on companion samples.

² Type 304L stainless steel was not used for the double U-bend specimens, because the type 304 and 316L stainless steels bound the range of SCC susceptible materials.

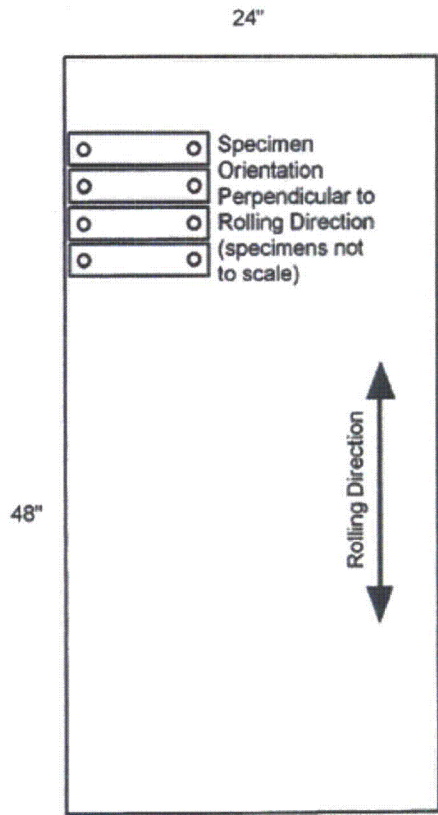


Figure 1 U-Bend Specimen Fabrication With Respect to the Sheet Rolling Direction (Specimen Dimensions not to Scale)

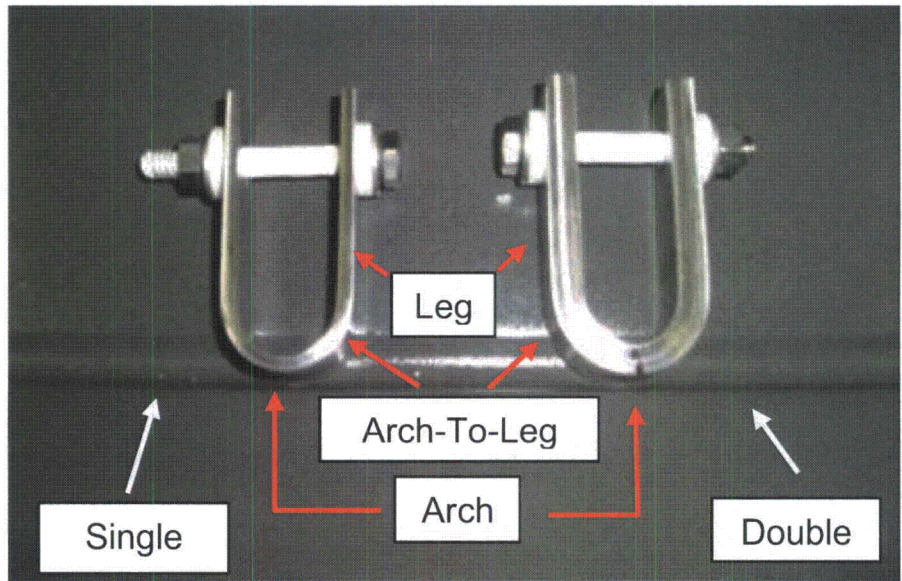


Figure 2 Configuration of the Single and Double U-Bend Specimens

Welded U-bend specimens were prepared from gas tungsten arc welded (GTAW) Type 304, 304L and 316L materials. The GTAW procedure was qualified to the requirements of the ASME Boiler and Pressure Vessel (B&PV) Code Section IX using a qualified welder (ASME, 2003a). Completed welds were examined by IHI Southwest Technology Inc., using a radiographic technique (RT) in accordance with the acceptance criteria in ASME B&PV Code Section III WB-5000 (ASME, 2003b). Materials that passed the ASME criteria were then machined into U-bend specimens with the weld crown located at the apex of the specimen outer surface, following both the ASTM G57 standard procedure (ASTM, 2005). Each welded U-bend specimen was inspected at a 50X magnification after bending to ensure that no cracks or fissures were present before testing.

2.1.2 Environmental Chambers

Figures 3 and 4 illustrate the standardized environmental chamber (Auto Technology model number CCT-NC-40) and the custom environmental chamber used for the SCC testing of the U-bend specimens. The standardized environmental chamber was used for the specimens held at or below 120 °C [248 °F] whereas the custom environmental chamber was used for the specimens held above 120 °C [248 °F]. The custom environmental chamber was made of 316L stainless steel and contained two spray nozzles at the top of the chamber. The standardized environmental chamber was equipped with two fogging towers and eight spray nozzles for enhanced spray/fog coverage. Before the test initiation, the chamber internal humidity sensor, dry bulb temperature, and bubble tower sensor were calibrated.

Each environmental chamber was equipped with horizontal test racks used to hold an array of tubular cartridge heaters, 1.905 cm [0.75 in] diameter and 45.72 cm [18 in] long, for heat supply to the U-bend specimens. Teflon[®] tape was wrapped around the cartridge heaters before the placement of the U-bend specimens. The temperature of each cartridge heater was controlled by a proportional-integral-derivative (PID) controller from Agilent (model number 34970A), shown in Figure 6. The inner radius of the apex curvature of the U-bends was in intimate contact with the cartridge heaters as shown in Figures 5 and 11.

To monitor the specimen temperature, selected U-bend specimens were mounted on each cartridge heater and instrumented with Type K thermocouples, as shown in Figure 5. A small hole was drilled at the specimen arch on the cross section of the U-bend, and a thermocouple was then inserted and kept in place with a silicone sealant. The temperature was monitored over time and stored in a portable computer (Figure 6). The temperature of each cartridge heater was then automatically adjusted to maintain the temperature of the instrumented thermocouple at the set point.

The temperature and relative humidity inside the environmental chambers were maintained within the target values by introducing a calibrated Vaisala[®] temperature and humidity probe (model number HM70) in the center of the chamber. The information obtained from the probe was used to modify the chamber set points in order to achieve the desired environmental conditions.



Figure 3 Picture of the Standardized Auto Technology Environmental Chamber



Figure 4 Picture of the Custom Stainless Steel Environmental Chamber

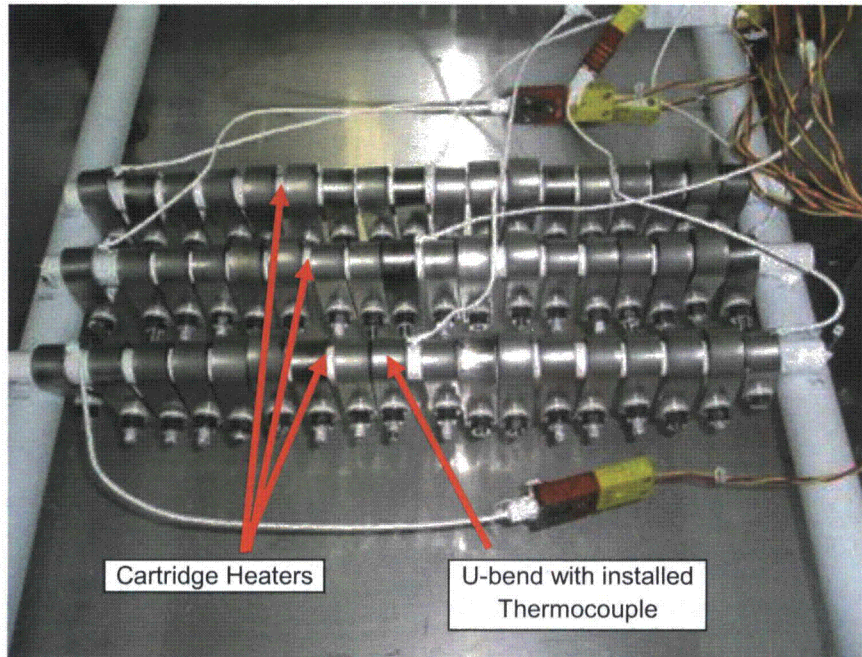


Figure 5 U-Bend Specimens Placed on Cartridge Heaters in the Custom Environmental Chamber



Figure 6 PID Controllers Used to Set and Control the Temperature of the Cartridge Heaters

For the first phase of the program, the salt spray testing was studied in both the standardized and custom environmental chambers. For the second phase of the program, the salt fog testing

was carried out only in the standardized environmental chamber, since the specimen temperatures were at or below 120 °C [248 °F] and this chamber is better suited to maintaining comparable environmental conditions among the specimens inside the chamber.

2.1.3 Salt Spray Testing Protocol

For the salt spray test, the conditions in the environmental chamber followed the guidelines of the General Motors (GM) 9540P accelerated corrosion test (General Motors, 1997) but with several modifications. The modified GM 9540P test procedure, shown in Table 2, consisted of four cycles of spraying the specimens with simulated sea salt for 15 sec, each followed by a 90 min hold time. Afterwards, a hold time of 209 min took place followed by a 480 min dry cycle. After the dry cycle, the procedure repeated itself starting with the spray cycle. Throughout the test, the chamber temperature was maintained at 25 °C [77 °F] and the relative humidity was allowed to fluctuate freely with the ambient conditions inside the chamber. The simulated sea salt used for the spray cycles was prepared according to the ASTM D 1141-98 (ASTM, 2003).

Table 2 Modified GM 9540P Accelerated Test Procedure for the Salt Spray Testing

Cycle Number	Cycle Description	Cycle Time
1	Spray with Simulated Sea Salt	15 sec
2	Hold at Current Conditions	90 min
3	Spray with Simulated Sea Salt	15 sec
4	Hold at Current Conditions	90 min
5	Spray with Simulated Sea Salt	15 sec
6	Hold at Current Conditions	90 min
7	Spray with Simulated Sea Salt	15 sec
8	Hold at Current Conditions	90 min
9	Hold at Current Conditions	209 min
10	Dry	480 min

Triplicate unwelded single and double U-bend specimens for each alloy were used. The specimen temperature was set to 25, 93, and 176 °C [77, 200, and 350 °F]. For the 25 °C [77 °F] specimens, the cartridge heaters were replaced by a 1.27 cm [0.5 in] Teflon[®] rod. Exposure times were set to 1, 2, 4, 7, 10, and 13 months. However, the test was discontinued 2 months after initiation due to the significant SCC noted in the majority of the specimens exposed at 93 °C [200 °F] and 176 °C [350 °F]. As discussed in Section 3, because of the observed temperature drop on the specimen during the direct application of the salt spray, the salt spray test environment proved to be extremely aggressive and more severe than what would be expected in dry storage cask environments.

As mentioned earlier, surface temperature of a material can have a significant effect on the surrounding environmental conditions, which ultimately affects the SCC susceptibility. To determine the severity of the salt spray test protocol, selected single and double U-bends were

instrumented with thermocouples at the specimen arch, arch-to-leg transition, and the leg regions for temperature profile determination (Figure 7). A total of three and six thermocouples were installed in single and double U-bend specimens, respectively.

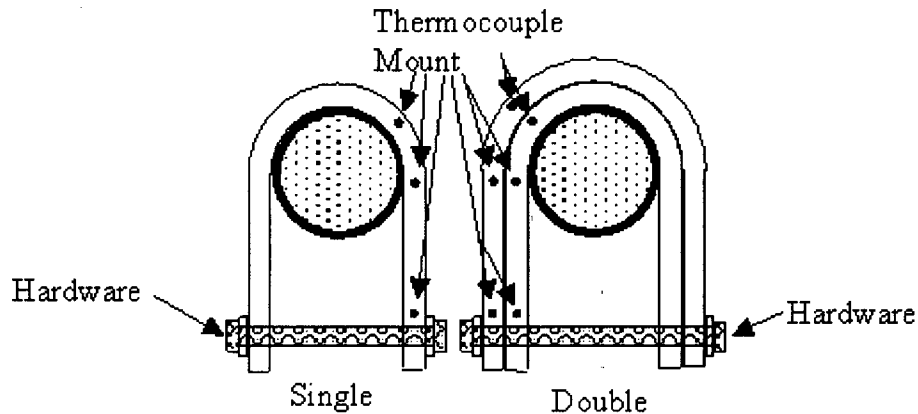


Figure 7 Schematics of the Locations of Thermocouples Attached to Selected Single and Double U-Bend Specimens for Temperature Profile Determination

2.1.4 Salt Fog Testing Protocol

As stated in Section 2.1.3, the salt spray test represents an extremely severe environment compared to in-service conditions of dry storage casks. As a result, a new salt fog test protocol was developed that was more representative of the actual environmental conditions expected for dry storage systems in coastal atmospheres.

The salt fog test was partitioned into two phases. The first phase was used to deposit an initial layer of salt on the surface of the U-bend specimens. The deposited salt is a necessary requirement for SCC development if the environmental conditions are propitious. To accomplish this, three salt deposition methods were studied. The first approach consisted of heating the U-bends to 70 °C [158 °F] on a hot plate followed by a light brushing of the specimen surface with a paintbrush previously impregnated with simulated sea salt. The second approach consisted of dipping the U-bends in a simulated sea salt solution at room temperature for about 10 sec followed by a drying period at 70 °C [158 °F]. Both approaches did not give a salt layer evenly deposited on the metal surface. Therefore, they were rejected.

An alternative salt deposition method was developed, which involved the exposure of U-bends at high temperatures while periodically fogging the surrounding environment with sea salt aerosols inside the standardized atmospheric chamber. The validation of this approach was studied on companion U-bends and was accomplished by cyclic fogging periods of 5 min using simulated sea salt followed by 15 min dry time. The cycle was repeated for 2 weeks. During this period, the U-bend specimens were maintained at 95 °C [203 °F] while keeping the chamber temperature at 30 °C [86 °F]. The resulting salt layer was evenly distributed over the specimen surface with slightly higher salt accumulation at the specimen arch. After deposition,

the salt was removed from the surface of these companion specimens, and the surface condition of the U-bends was examined to ensure that the deposited salt did not lead to crack formation, localized corrosion, or uniform corrosion. Based on favorable visual observations, this method was then adopted during the first phase of the salt fog test. Figure 8 shows an image of the half U-bend samples after the salt deposition phase.

Immediately after the conclusion of the salt deposition phase and without removing the specimens from the chamber, the accelerated corrosion testing phase started, exposing the specimens to a continuous high humidity and dry cycles with periodic salt deposition cycles at selected times (see Table 3). The salt fog test was significantly different from the previously described salt spray test. Dry deposition of sea salts was accomplished using short salt fog periods. In addition, this test protocol subjected the specimens to changes in relative humidity to allow deliquescence and efflorescence of the deposited salts to occur while maintaining or increasing the amount of salt accumulated on the specimen surface.

As shown in Table 3, the salt fog test protocol consisted of four 5 min salt fogging cycles each followed by a 60 min ambient cycle. During the ambient cycle, the chamber was allowed to reach a pseudo equilibrium state based on the environmental conditions that resulted from the previous cycle. This part of the protocol was used to maintain a thin salt layer on all the specimens throughout the exposure time necessary for continuing SCC development. Following the salt fog deposition periods, alternating dry and high humidity cycles were applied to represent conditions of low and high relative humidities associated with diurnal temperature and humidity variations in field applications. The dry cycle was carried out for 100 min by pulling moist air out of the chamber and replacing it with dry air. During the salt fog, ambient, and dry cycles, the chamber internal temperature was set to 30 °C [86 °F]. Two cycles (10 and 11) with increased humidity levels at 30 °C [86 °F] followed. The first increase in humidity during cycle 10 (Table 3) was carried out for 125 min and was accomplished by filling the bottom of the chamber with deionized water. For the second 55 min high humidity cycle, the deionized water in the bottom of the chamber was heated to 52 °C [126 °F], which increased both the chamber relative humidity and temperature. The environmental chamber settings, which controlled the temperature set points of the chamber heaters, had to be adjusted in order to obtain a target high humidity above 70 percent, while maintaining the temperature of the U-bend specimens at ± 5 °C [± 9 °F] from their desired temperatures. After the high humidity cycle, a 180 min dry cycle was repeated at the end of the test protocol. Throughout the salt fog test, the relative humidity was allowed to fluctuate freely with the ambient conditions inside the chamber. The entire cycling sequence was repeated twice a day for 52 weeks.

Table 3 Accelerated Corrosion Cycles of the Salt Fog Test

Cycle Number	Chamber Cycle	Cycle Time, min	Cycle Description
1	Salt fog	5	Deposit salt on the specimens
2	Ambient	60	
3	Salt fog	5	
4	Ambient	60	
5	Salt fog	5	
6	Ambient	60	
7	Salt fog	5	
8	Ambient	60	
9	Dry	100	Low relative humidity
10	Increase humidity	125	Increase relative humidity in chamber
11	High humidity	55	Highest relative humidity
12	Dry	180	Low relative humidity

The salt fog test was carried out for 4, 16, 32, and 52 weeks of exposure, using triplicate specimens for each specimen type. Prior to testing, the specimens were mounted on cylindrical tubular heaters inside the test chamber as described in Section 2.1.2. Each cartridge heater accommodated 16 specimens and 2 half U-bend samples for temperature control and salt deposition rate measurements (Figure 9). The 16 specimens were comprised of two unwelded single and two welded single U-bend specimens for each of the 304, 304L, and 316L materials, and two double U-bend specimens for each of the 304 and 316L materials.

After the initial salt deposition was completed and during the first week of testing, the U-bend target temperatures were originally set to 43, 95, and 135 °C [109, 203, and 275 °F]. However, due to the high thermal mass resulting from the small chamber volume compared to the total surface area of the test specimens, the chamber relative humidity would not increase above a value of 70 percent. Therefore, the temperature of the 95 and 135 °C [203 and 275 °F] specimens was decreased to 85 and 120 °C [185 and 248 °F] for the remainder of the test.

Figure 10 shows a schematic of the layout of the heaters inside the chamber and a representative picture of the experimental setup of the salt fog test. As shown in Figure 11, the inner surface of the specimen arch was positioned facing upward in close contact with the heater perimeter so that salt could accumulate on the outer specimen surface where increased stress concentration was expected.



Figure 8 Typical Appearance of the Half U-Bend Samples Used for Salt Deposition Measurements After 2 Weeks of Exposure

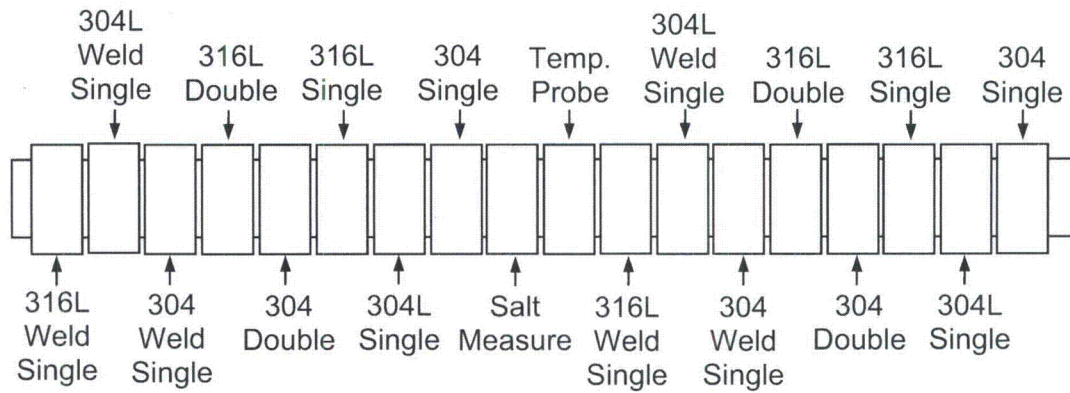


Figure 9 Schematic of the U-Bend Specimen Arrangement on Each Cartridge Heater

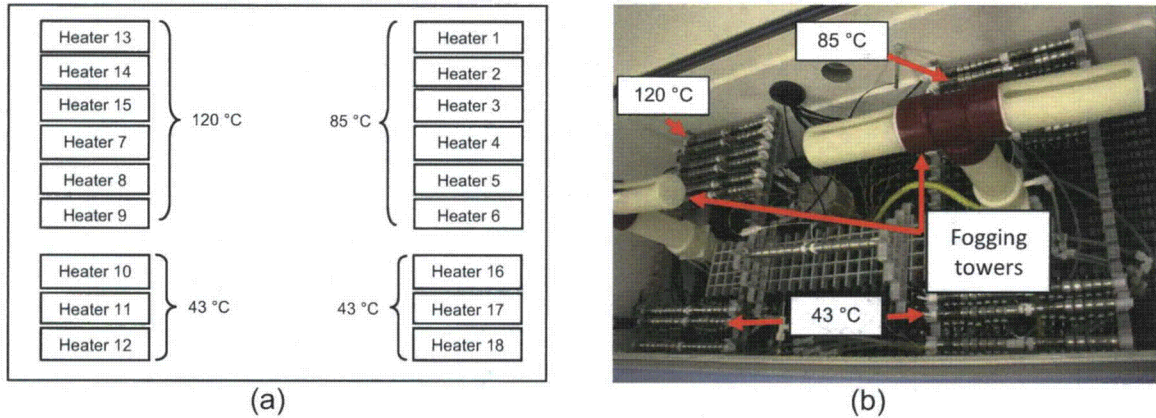


Figure 10 (a) Schematic of the Cartridge Heater Layout and (b) a Picture of the Standardized Atmospheric Chamber

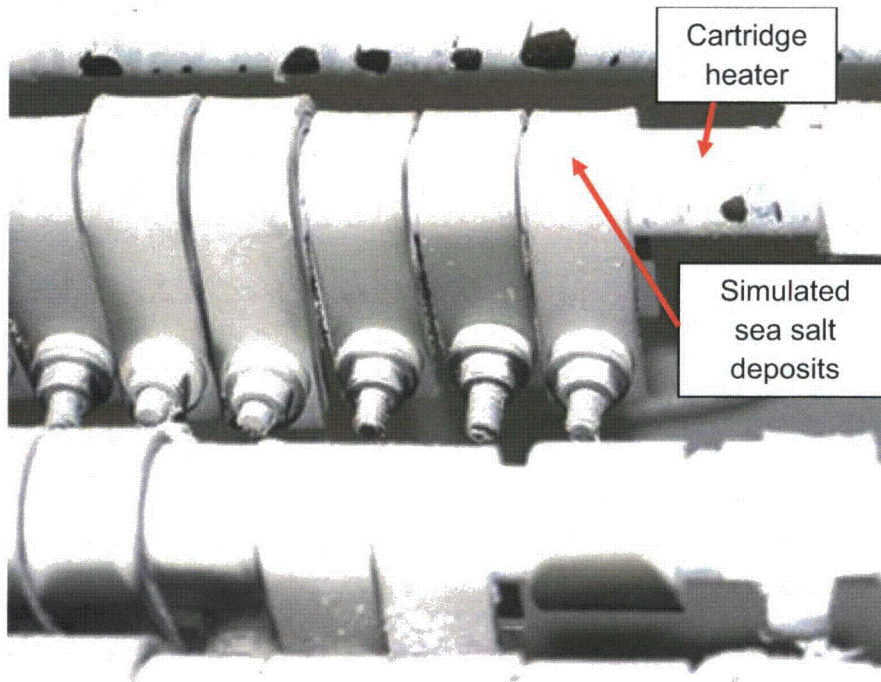


Figure 11 Typical U-Bend Arrangement Used for the Salt Spray and Salt Fog Tests

2.1.5 Examination of SCC

In order to determine if cracking events were purely the consequence of the stress/solution/environment interaction, rather than being attributed to the bending process, each U-bend specimen was examined to ensure that no cracking was present before testing. After each exposure time, the U-bend specimens were photographed and cleaned in an ultrasonic bath filled with distilled water followed by cleaning with isopropyl alcohol and diluted hydrochloric acid. Afterwards, all the specimens were inspected using an optical microscope

(Olympus PMG3) with a resolution of 50X. If cracks were not found at that magnification, the suspected specimens were examined at a 500X magnification.

2.1.6 Salt Chemical Composition and Deposition Rates

The nature of the salt composition will affect its deliquescence (and efflorescence) behavior, which is closely related to the SCC susceptibility. Samples of salt were collected at selected times from the surface of several of the U-bend test specimens at each test temperature. Samples were stored in tightly sealed plastic bags. The salt composition was determined using both inductively coupled plasma mass spectrometry and ion chromatography techniques. Seawater solutions of known composition were also obtained from the Gulf of Mexico near Corpus Christi, TX and used for calibration and verification of the testing devices.

In order to determine the salt deposition rates before the salt fog test, a 6-week test was initially examined using 304 stainless steel flat specimens of the same dimensions as the half U-bend samples. The flat specimens were placed inside the chamber and heated to 43, 85, and 120 °C [109, 185, and 248 °F]. The chamber temperature and relative humidity were set to 35 °C [95 °F] and 25 percent, respectively, which corresponded to an absolute humidity of 10 g/m³ [3.61 10⁻⁷ lb/in³]. Each salt fog cycle was 5 min long carried out every 20 min for a total of 3 cycles/hr. A picture of the 85 °C [185 °F] specimens during testing is shown in Figure 12.

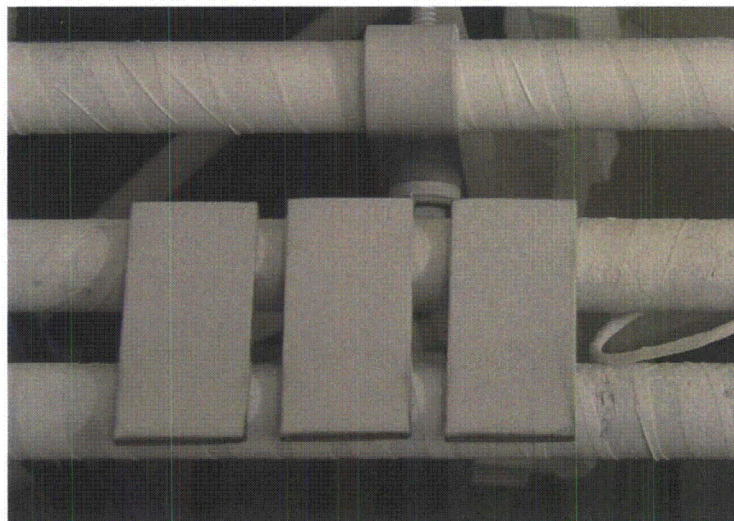


Figure 12 Photograph of the Flat Specimens Exposed to 85 °C [185 °F] Used for the Salt Deposition Rate Determination. The Specimens Appeared to be Completely White Because of the Deposited Salt

Salt deposition rates were computed as follows:

$$\text{Salt deposition rate / mg m}^{-2} \text{ day}^{-1} = (W_S - W_C) A^{-1} t^{-1} \quad (1)$$

where W_S and W_C are the specimen weights before and after salt removal, respectively, A is the one-sided specimen area, and t is the exposure time.

During the actual execution of the salt fog test, salt deposition rates were computed over time using half U-bend samples mounted on the cartridge heaters at the beginning of the exposure (Figure 8). At selected exposure times, a single half U-bend sample at each temperature was extracted from the chamber and immediately weighed before salt removal to avoid salt deliquescence. Then, the salt was removed from the half U-bend surface with deionized water, and the sample was dried and weighed to determine the weight change. The weights were taken using an analytical balance with an accuracy of 0.1 mg [$3.53 \cdot 10^{-6}$ oz].

2.2 SCC Complementary Testing

In order to develop a more realistic, yet still conservative accelerated SCC test, additional experiments were carried out. These experiments gave a better understanding of the underlying processes controlling SCC of the specimens exposed during the salt fog test and the environmental conditions associated with salt deliquescence necessary for SCC. Tests were carried out to: (1) measure the environmental relative humidity and temperature profiles surrounding a heated U-bend specimen, (2) determine the salt deliquescence and efflorescence points, and (3) evaluate SCC under various controlled humidity/temperature conditions other than those examined in the atmospheric chamber.

2.2.1 Environmental Temperature and Humidity Profiles

In order to understand the environmental properties surrounding a loaded spent fuel canister, a temperature-humidity profile was studied around a heated U-bend specimen. The test was done by heating multiple U-bend specimens to 60, 70, 80, 94, and 120 °C [140, 158, 176, 201, and 248 °F] in the environmental chamber. The chamber relative humidity and air temperature were held at 95 percent and 35 °C [95 °F], respectively. Using calibrated calipers and a Vaisala® temperature/humidity probe, the relative humidity, absolute humidity, and temperature were measured at various distances from the arch of the U-bend to the centerline of the Vaisala® probe where the sensor is located, both in the horizontal and vertical directions.

2.2.2 Salt Deliquescence and Efflorescence

Salt deliquescence and efflorescence as a function of relative humidity and salt composition were determined at 50 and 80 °C [122 and 176 °F]: Four salt samples tested included a certified reagent grade sodium chloride, anhydrous magnesium chloride, simulated sea salt, and a sample of sea salt collected from the Gulf of Mexico near Corpus Christi, TX. The sea salt from the Corpus Christi was filtered through a 0.22 µm [8.66 µin] filter paper before solution evaporation. Salt samples were weighed and transferred to glass beakers placed inside an

ESPEC humidity chamber (model number ETH2). The chamber relative humidity was varied from 20 percent up to 80 percent in 5 percent increments during a period of 24 hr. Visual observation of the salts was carried out for each relative humidity increment.

2.2.3 Controlled Relative Humidity/Temperature Tests

In order to evaluate the environmental relative humidity and temperature conditions leading to SCC besides those examined in the standardized environmental chamber, additional tests were carried out in the ESPEC humidity chamber. Companion 304 stainless steel half U-bend samples were placed with the outer surface of the arch facing upward as in the actual testing.

Before this test, simulated sea salt was deposited on half U-bend samples, following the procedure described in Section 2.1.4. After the initial salt deposition, the half U-bend samples were placed in the humidity chamber at various temperature and relative humidity combinations (see Table 4) for 1-month and 2-month exposures. Concurrently, additional testing was carried out to determine the effect of solution chemistry on SCC development. Three different liquid droplet compositions were examined: sodium chloride, magnesium chloride, and simulated sea salt. At the beginning of the exposure, one 500- μ L solution droplet of the trial solution composition was placed on the arch of a salt-free half U-bend specimen. Several specimens of each droplet composition were manufactured for testing at relative humidities of 40, 50, and 65 percent. The test was carried out for up to 2 months at 50 °C [122 °F]. After exposure, the samples were photographed and examined by optical microscopy. A laser profilometer (Z-Scope) with wavelength of 632 nm and vertical and lateral resolutions of 0.5 μ m and 1 μ m [19.7 μ in and 39.4 μ in], respectively, was used to scan the surface of the U-bends to determine the topography associated with surface degradation after exposure.

Table 4 Temperature and Relative Humidity Parameters of the Controlled Relative Humidity/Temperature Tests

Temperature, °C [°F]	Relative Humidity, %
65 [149]	70
50 [122]	65
50 [122]	50
50 [122]	40

3 SALT SPRAY TESTING RESULTS

This section presents the results of the U-bend testing in the modified GM 9540P test procedure described in Section 2.1.3. The results include cracking data of 304, 304L, and 316L stainless steel single and double U-bend specimens exposed to the GM 9540P for 1-month and 2-month exposure periods. Initially, three U-bend specimens for each alloy were placed in the chamber for 1-month and 2-month exposure periods.

3.1 U-Bend Specimens Held At 25 °C [77 °F]

Optical examination of the single and double U-bend specimens that were held at 25 °C [77 °F] showed minor corrosion distress for the 304 stainless steel, but no signs of cracking for all the alloys for both 1-month and 2-month exposure periods. This observation was consistent with the specimen temperature being lower than the expected critical temperature for SCC development.

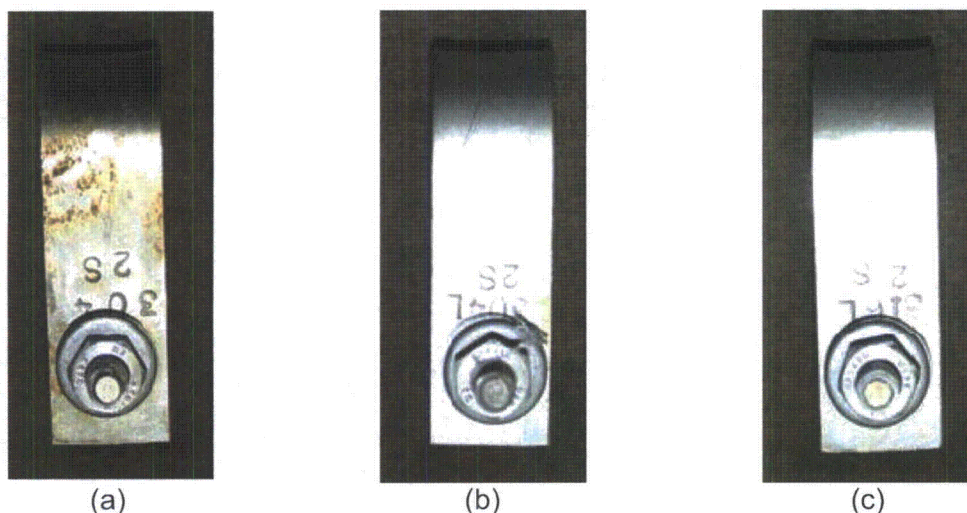


Figure 13 Typical Surface Appearance of the Single U-Bend Specimens: (a) 304, (b) 304L, and (c) 316L Held at 25 °C [77 °F] for a 1-Month Exposure

3.2 U-Bend Specimens Held At 93 °C [200 °F]

Specimens held at 93 °C [200 °F] and exposed to the salt spray for 1 month showed evidence of cracking for all the alloys. For instance, all six 304 stainless steel single and double U-bend specimens showed cracking in the legs, leg-to-arch transition, and arch regions. Figure 14 shows examples of the typical stress corrosion cracking of both the single and double U-bend specimens exposed for 1 month. The 304L stainless steel single U-bends also showed cracks along the whole length of the material as illustrated in Figure 15. The SCC behavior of the 316L stainless steel U-bend specimens was different from the 304 and 304L stainless steels. Only one of the 316L stainless steel single U-bend specimens cracked 1 month after exposure (Figure 16). However, cracking was observed on all three of the 316L double U-bend

specimens. On one of these U-bend specimens, cracking was only observed on the inner U-bend specimen. This is likely due to the crevice retaining residual salt solution. However, the other two 316L double U-bends had cracking on both the inner and outer U-bend specimens. Additionally, cracking did not occur in the arch region for the 316L samples and was restricted to the leg and arch-to-leg transition regions.

The amount of cracking increased for the 2-month exposure for the specimens held at 93 °C [200 °F] compared to that observed during the 1-month exposure. All six of the 304 stainless steel single and double U-bend specimens showed SCC, located along the whole length of the specimen. Similarly, all three of the 304L stainless steel single U-bends cracked after 2 months. Interestingly, none of the specimens cracked in the arch region but only along the leg and the leg-to-arch transition regions. All three of the 316L stainless steel single and double U-bend specimens showed stress corrosion cracks after 2 months. Cracking was limited to the leg and arch-to-leg transition regions and both the inner and outer U-bend regions. A few cracks were observed in the arch region of the 316L stainless steel double U-bend specimens, but these were only found in the crevice region.

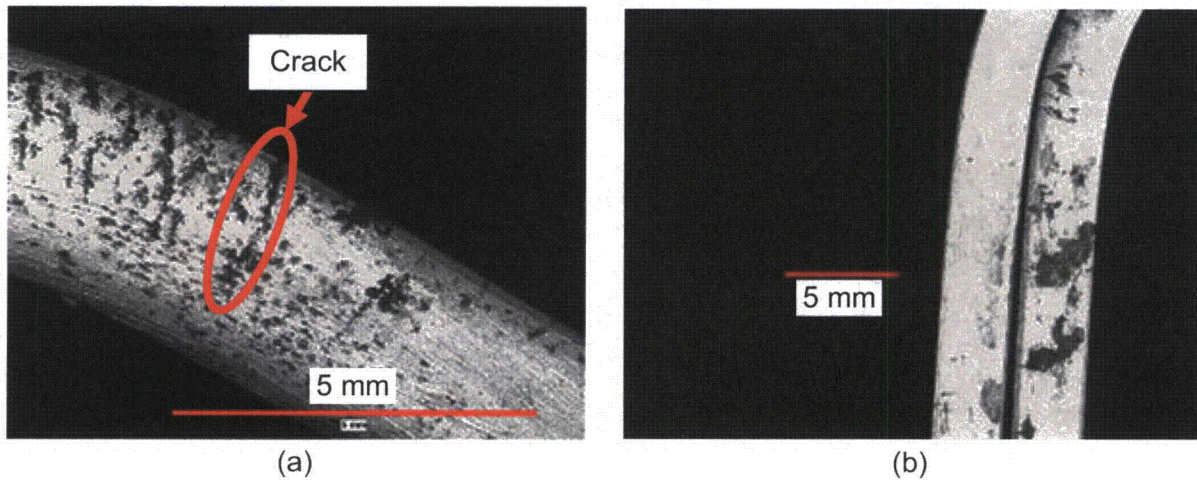


Figure 14 Typical SCC Behavior of the 304 Stainless Steel (a) Single and (b) Double U-Bend Specimens Exposed for 1 Month at a Temperature of 93 °C [200 °F]

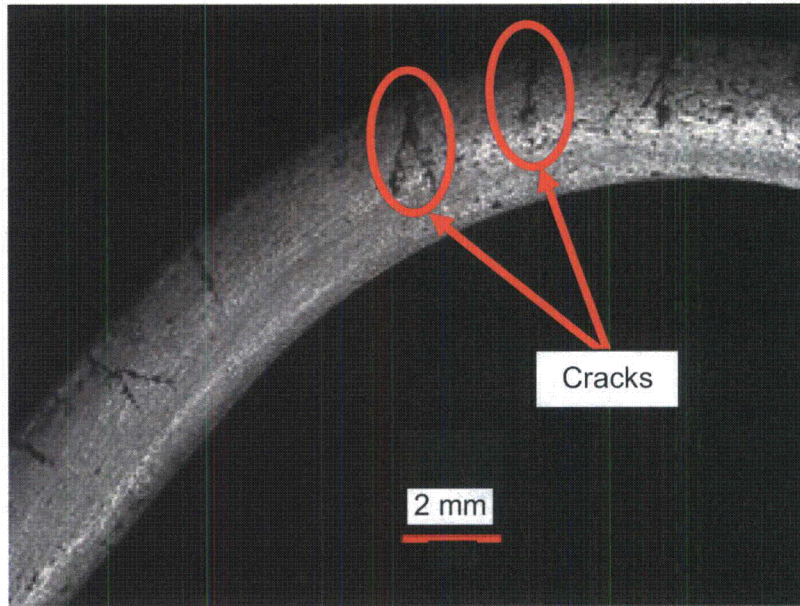


Figure 15 Typical SCC Behavior of a 304L Stainless Steel Single U-Bend Specimen Exposed for 1 Month at a Temperature of 93 °C [200 °F]

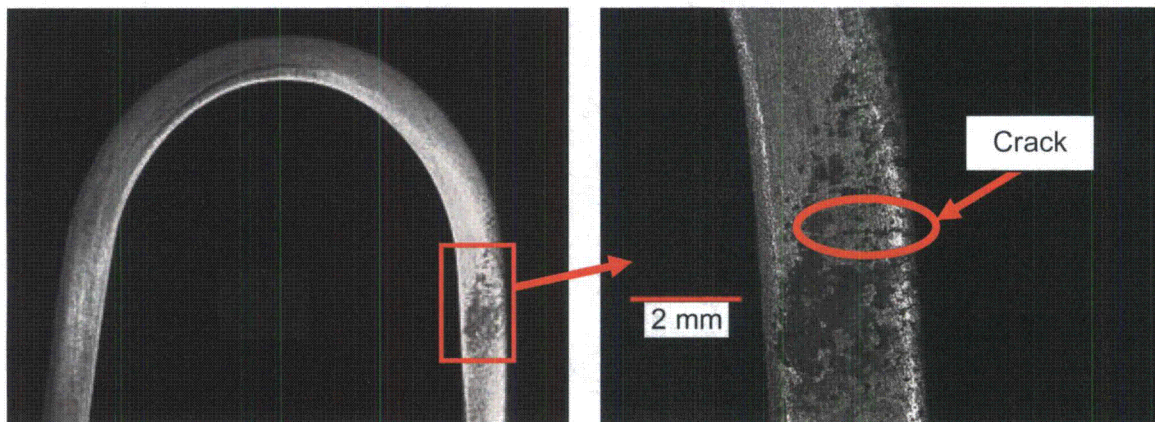


Figure 16 Typical SCC Behavior of a 316L Stainless Steel Single U-Bend Specimen Exposed for 1 Month at a Temperature of 93 °C [200 °F]

3.3 U-Bend Specimens Held At 176 °C [350 °F]

The U-bend specimens held at 176 °C [350 °F] exposed to the salt spray for 1 month showed evidence of cracking in some of the alloys. For instance, one of three 304 stainless steel single U-bends and all of the 304 stainless steel double U-bend specimens showed cracking in the leg region as shown in Figures 17 and 18. Moreover, two of the three 316L stainless steel single U-bends showed evidence of SCC in the leg region. Similarly, two of the three 316L stainless steel double U-bend samples showed the occurrence of SCC. The cracks observed on the 316L double samples were only located on the inner U-bend sample in the legs or arch-to-leg

transition regions. An image of the SCC that occurred on the inner U-bend sample for the 316L stainless steel double samples is shown in Figure 19. On the other hand, no SCC was observed in any of the 304L stainless steel single U-bends.

As expected, the amount of SCC on the specimens exposed for 2 months increased compared to that observed for 1 month. All of the 304 stainless steel single and double U-bends developed SCC, limited to the leg region for the single U-bend specimens and along the arch-to-leg transition and the leg regions for the double specimens. All three of the 316L stainless steel single and double U-bends showed SCC, limited to the arch-to-leg transition and leg regions for the single U-bend specimens. The cracks observed on the double specimens were located on the leg region for the outer specimens and in both the leg and arch-to-leg transition regions for the inner specimens. On the other hand, only one of the 304L stainless steel U-bends showed signs of SCC concentrated around the arch-to-leg transition region.

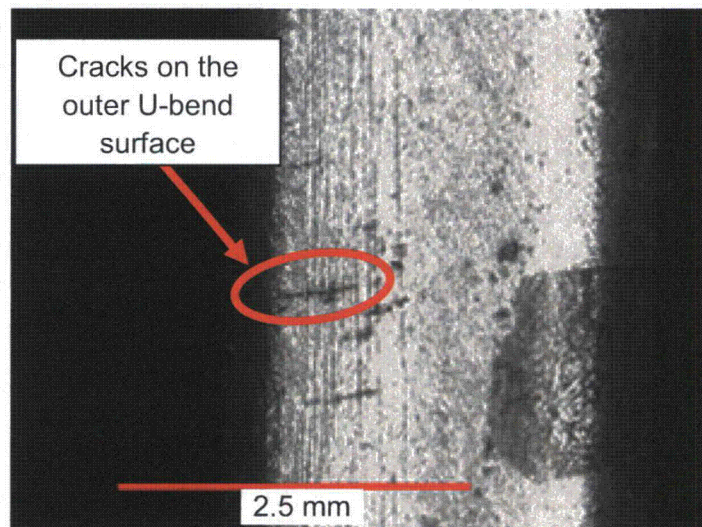


Figure 17 Typical SCC Behavior of a 304 Stainless Steel Single U-Bend Specimen Exposed for 1 Month at a Temperature of 176 °C [350 °F]

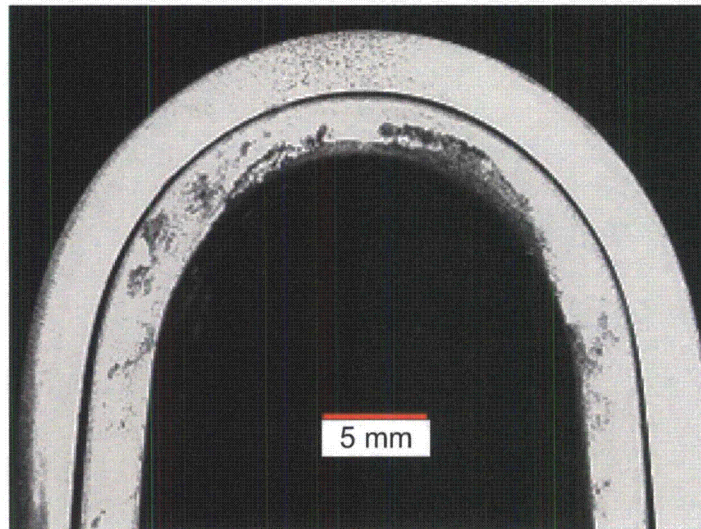


Figure 18 Typical SCC Behavior of a 304 Stainless Steel Double U-Bend Specimen Exposed for 1 Month at a Temperature of 176 °C [350 °F]

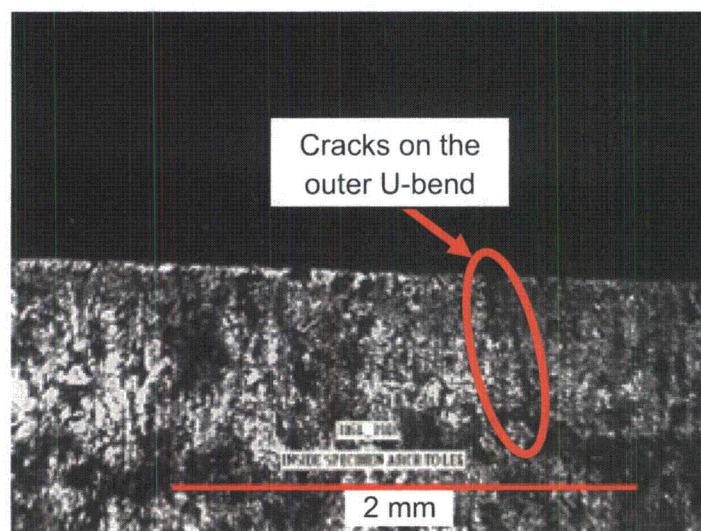


Figure 19 Typical SCC Behavior of the Inner 316L Stainless Steel Double U-Bend Specimen Exposed for 1 Month at a Temperature of 176 °C [350 °F]

3.4 Discussion

As mentioned earlier, surface temperature of a metal plays a key role in the susceptibility to stress corrosion cracking. The temperature affects the surrounding environment properties (discussed in Section 5), the evaporation rate of any liquid in contact with the surface, and the activation energy for SCC initiation. SCC was not observed on any of the specimens held at 25 °C [77 °F]. This observation is in agreement with those reported by Truman (1977), where below a temperature of roughly 45 °C [113 °F], SCC was not observed in 304 stainless steel exposed to sodium chloride at pH of 2. In the current effort, SCC was observed on the U-bend

specimens that were held at temperatures of either 93 °C [200 °F] or 176 °C [350 °F]. It was expected that the 93 °C [200 °F] samples would have some form of SCC because the temperature was below the boiling point of simulated sea salt but high enough for SCC initiation. This temperature allows the salt to remain in solution on the surface of the samples leading to an environment where SCC can occur. However, it was not expected that SCC would be observed on any of the samples held at 176 °C [350 °F]. At these temperatures, the water present in the simulated sea salt was expected to have boiled quickly from the surface of the samples, leaving behind a dry salt on the metal surface. This scenario would not allow the necessary environment to develop that could lead to SCC. In order to examine how the temperature may have affected the SCC susceptibility of the U-bend samples, both single and double U-bend samples were machined and fitted with thermocouples to measure the temperature profile between the arch and leg of the samples. As can be seen in Figure 7, temperature probes were affixed to the U-bend samples in the leg, arch-to-leg transition, and arch regions. For the double U-bend sample, temperature probes were placed in the same three areas, in both the inner and outer U-bend elements. The temperature profiles were measured using the same modified GM 9540P procedure used for the U-bend SCC tests described in Section 2.1.3.

The results of the temperature profile testing for the 93 °C [200 °F] and 176 °C [350 °F] U-bend specimens exposed to the salt spray test are shown in Figures 20 and 21. During the test, there was a temperature gradient (~3 °C [~37 °F] for the 93 °C [200 °F] specimens and ~20 °C [~68 °F] for the 176 °C [350 °F] specimens) between the legs and the arch of the U-bends. The specimen legs, which were not in contact with the heating element, acted as fins cooling off the U-bend specimens. In addition to the temperature gradient, there was a significant temperature decrease in the U-bends (roughly 32 °C [90 °F] for the 93 °C [200 °F] specimens and 80 °C [175 °F] for the 176 °C [350 °F] specimens) during the salt spray cycles. The temperature drop was related to the deposition of the salt solution, sprayed at 25 °C [77 °F], on the U-bend specimen surface. This temperature drop allowed the simulated sea salt to remain in solution on the surface of the U-bends for a certain period after each spray cycle. It is expected that the simulated sea salt deposited on the low temperature specimens would remain in solution longer than it normally would at elevated specimen temperatures. The temperature gradient along the length of the U-bend specimens likely led to the leg regions being in contact with the simulated salt solution for a longer period. It is suspected that this is the reason why more cracking was observed in the leg and leg-to-arch transition regions than in the arch of the U-bends held at either 93 °C [200 °F] or 176 °C [350 °F].

In summary, the environment in the salt spray test was extremely aggressive and promoted rapid SCC in the austenitic stainless steels. Moreover, this environment is not representative of actual service conditions of dry storage canisters. As a result, the salt fog test was developed to minimize the temperature drop over the entire U-bend surface observed during the spray operation. While the temperature gradient from the arch to specimen leg will still be present, it should be decreased by the insulation provided by the deposited salt. More importantly, the large temperature drop that occurs when the spray impinges on the specimen (Figure 20) is

eliminated in the salt fog test. In addition, the salt fog test was developed as a more representative, yet still functions as an accelerated test of field conditions for dry storage system canisters. The results of the salt fog testing are presented in Section 4.

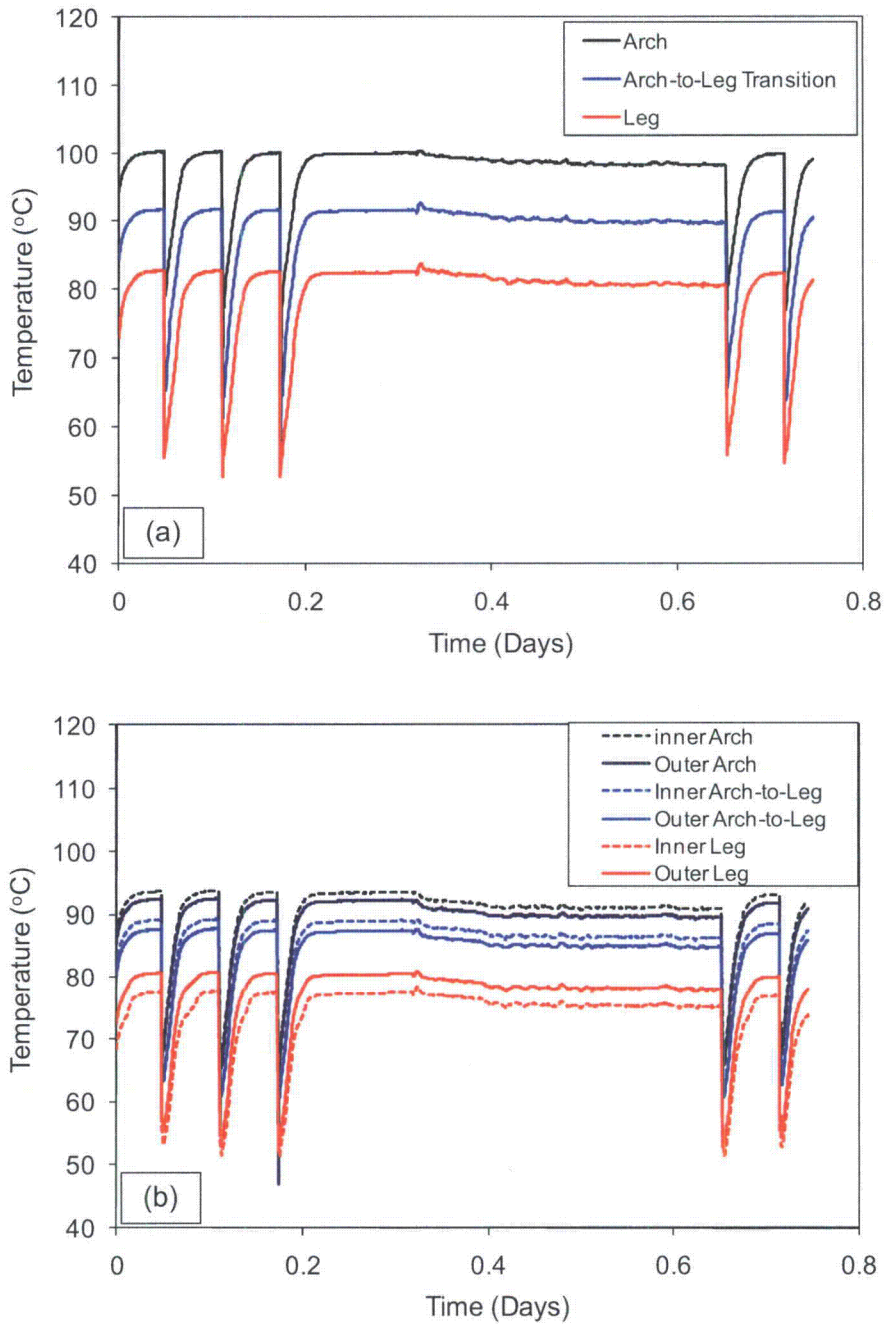


Figure 20 Temperature Profile for a) Single and b) Double U-Bend Specimens at 93 °C [200 °F] Subjected to the Salt Spray Test

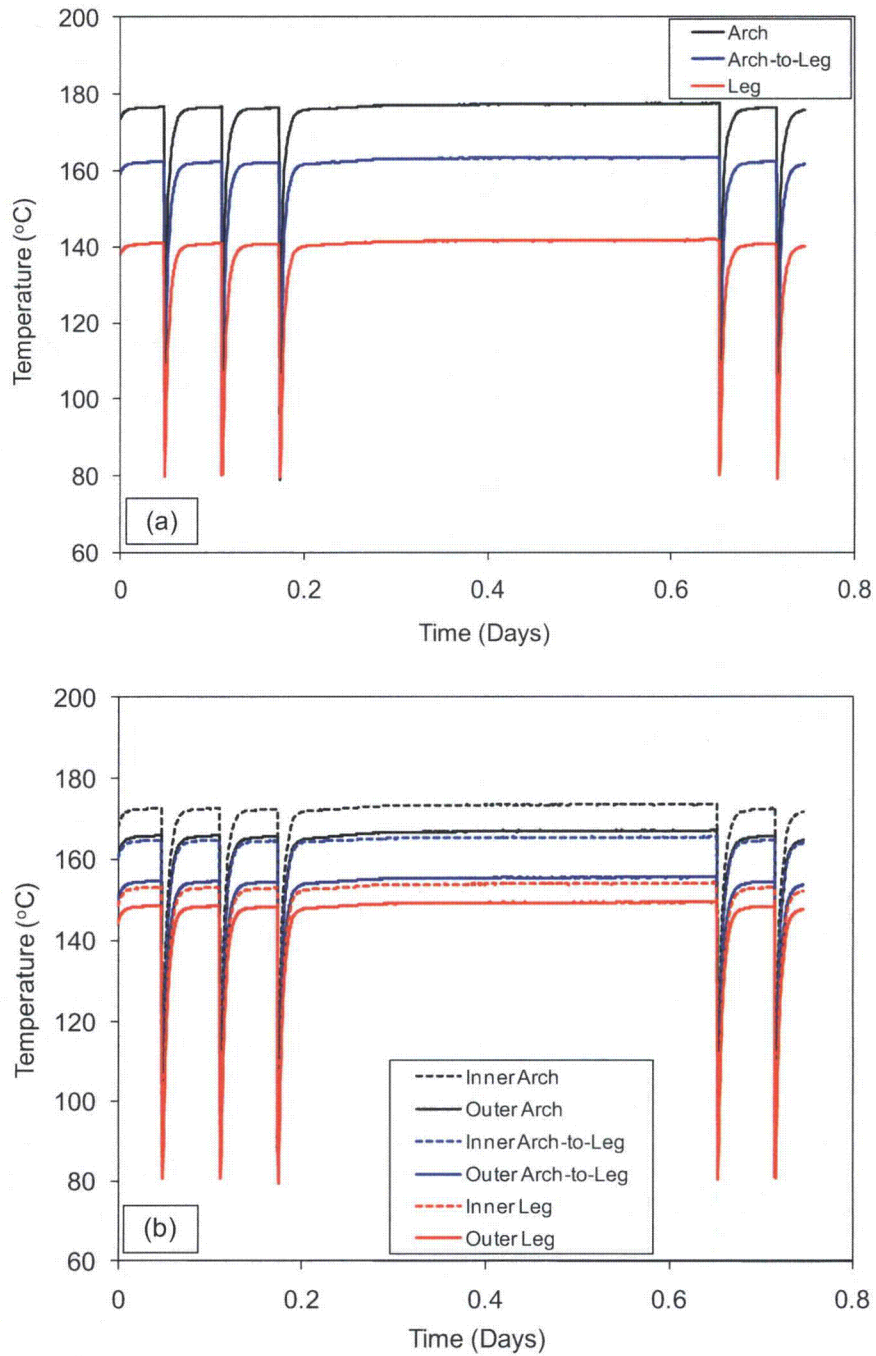


Figure 21 Temperature Profile for a) Single and b) Double U-Bend Specimens at 176 °C [350 °F] Subjected to the Salt Spray Test

4 SALT FOG TESTING RESULTS

In this section, results of the U-bend testing using the salt fog test protocol, described in Section 2.1.4, are presented. The results include data for the 304, 304L, and 316L stainless steel single, double, and welded U-bend specimens evaluated at 4, 16, 32, and 52 weeks after test initiation. During the first week of testing, the U-bend target temperatures were set to 43, 95, and 135 °C [109, 203, and 275 °F]. As mentioned earlier, the large thermal mass of the specimens placed inside the chamber did not allow the relative humidity to increase above the target value of 70 percent for the simulated sea salt to deliquesce. Therefore, the temperature of the 95 and 135 °C [203 and 275 °F] specimens was slightly modified to 85 and 120 °C [185 and 248 °F]. This temperature change was not expected to produce significant differences in the SCC behavior compared with the previous temperature targets. During the entire exposure time, the temperatures of all the 85 and 120 °C [185 and 248 °F] specimens were constant. The temperature of all the 43 °C [109 °F] specimens were also constant during the cycles 1 to 10 and 12 (fogging, ambient, increase humidity, and dry cycles), and increased to 48 °C [118 °F] for a few minutes during the cycle 11 (high humidity cycle) due to an increase in chamber temperature.

Initial optical examination at a 500X magnification did not reveal the presence of cracks in all the specimens before exposure. For the 4-week exposure, the 43, 85, and 120 °C [109, 185, and 248 °F] specimens were taken from heaters 10 and 11, 1 and 2, and 13 and 14, respectively. For the 16-week exposure, the 43, 85, and 120 °C [109, 185, and 248 °F] specimens were taken from heaters 11 and 12, 2 and 3, and 14 and 15, respectively. For the 32-week exposure, the 43, 85, and 120 °C [109, 185, and 248 °F] specimens were taken from heaters 16 and 17, 4 and 5, and 7 and 8, respectively. For the 52 weeks of exposure, the 43, 85, and 120 °C [109, 185, and 248 °F] specimens were taken from heaters 17 and 18, 5 and 6, and 8 and 9, respectively. A total of 72 U-bend specimens were removed at each exposure period. After removal of the U-bend specimens from the atmospheric chamber at each exposure time, the corresponding heaters were not turned off so that the internal temperature, absolute humidity, and relative humidity trends remained nearly constant throughout the test exposure.

Figure 22 shows typical temperature, relative humidity, and absolute humidity trends of the bulk environment inside the chamber as a function of time for two consecutive full cycles as shown in Table 3. The trends are characterized by four transient sharp peaks in the relative and absolute humidity values spaced each other about 1 hr, consistent with the occurrence of the four fog cycles in Table 3. During that period, the relative humidity varied from 35 percent to 60 percent and the absolute humidity from 15 g/m³ [5.42 10⁻⁷ lb/in³] to 28 g/m³ [1.01 10⁻⁶ lb/in³]. Also during that period, the temperature in the chamber gradually increased from 35 °C [95 °F] to 43 °C [109 °F]. Afterwards, both the relative and absolute humidity values decreased to 22 percent and 8 g/m³ [2.89 10⁻⁷ lb/in³], respectively, in agreement with the occurrence of the dry cycle. Following the low humidity cycle, a two-fold increase in relative and absolute humidity took place, reaching 75 percent and 60-65 g/m³ [2.16-2.35 10⁻⁶ lb/in³], respectively. The temperature in the chamber during the high humidity cycle also increased temporarily to 52 °C [126 °F] for a

few minutes. Afterwards, the temperature, relative and absolute humidity values decreased to 35 °C [95 °F], 22 percent, and 8 g/m³ [2.89 10⁻⁷ lb/in³], respectively, during the last dry cycle of the protocol.

As in the salt spray test, the presence of a temperature gradient between the arch and the legs of the U-bend specimens during the salt fog test was likely. However, because the large temperature drop does not occur during the salt fog cycles (as explained in Section 3.4), the temperature gradient was not expected to affect the development of SCC. This expectation was confirmed by the fact that any cracking observed during the salt fog tests occurred at the specimen apex (where residual stresses are highest) and not in the apex-to-leg transition region as in the higher temperature salt spray tests.

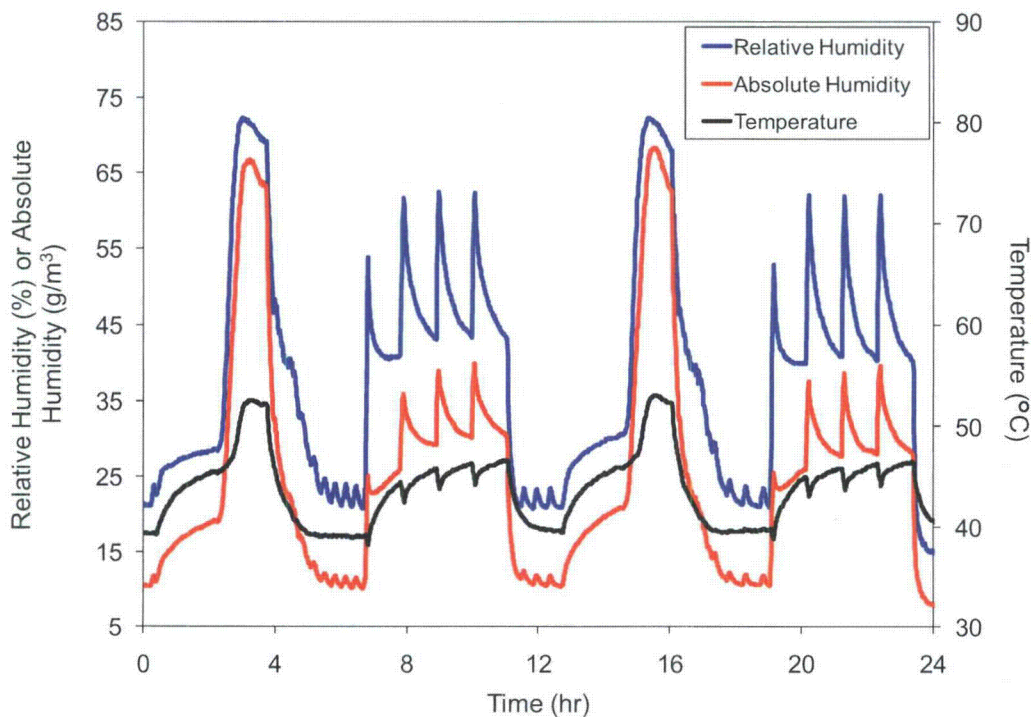


Figure 22 Chamber Temperature, Relative Humidity, and Absolute Humidity Trends as a Function of Time for Two Consecutive Full Cycles Recorded During the Salt Fog Test

4.1 U-Bend Specimens Held At 43 °C [109 °F]

4.1.1 Results of the 4-Week Exposure Time

The surface of all the U-bend specimens exposed to 43 °C [109 °F] for 4 weeks showed a combination of a thin salt layer as well as formation of corrosion products. Salt deposits were mostly found at the apex curvature of the bend. The 304 and 304L, welded and unwelded, single and double U-bend specimens exhibited accelerated damage in the form of large pits and

general corrosion at the apex curvature of the bend, particularly within the weld and heat-affected zone in the welded specimens. The 316L single and double weld and unwelded U-bend specimens showed less corrosion deposits than the 304 and 304L specimens did, but pitting corrosion was noted at the heat-affected zone and none at the weld area. For all the single U-bend specimens, the presence of isolated small pits (and edge corrosion for the 304 and 304L specimens) were more noticeable at the bent apex curvature area. For all the double U-bend specimens, corrosion was more prominent in the outer specimen compared to the inner specimen, which showed only corrosion at the edges. After exposure, most of the corrosion products and deposited salt were removed during cleaning. After cleaning, optical examination at 100X magnification showed the presence of small and tight cracks ($<3\ \mu\text{m}$ wide) in one unwelded 304 and 304L single and double U-bend specimens. On the contrary, optical examination of all the 316L U-bends showed no apparent cracks. Pictures of the typical surface appearance of the $43\ \text{°C}$ [$109\ \text{°F}$] U-bend specimens inside the atmospheric chamber after 4 weeks of exposure are shown in Figure 23.

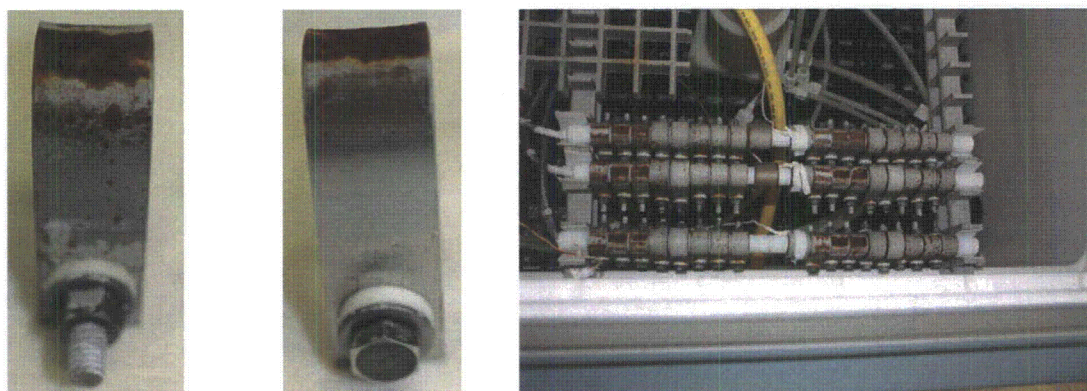


Figure 23 Pictures of Selected $43\ \text{°C}$ [$109\ \text{°F}$] 304 and 304L Weld U-Bend Specimens and an Overall Photograph of all the $43\ \text{°C}$ [$109\ \text{°F}$] Specimens Mounted on the Heaters 16, 17, and 18 in the Environmental Chamber After 4 Weeks of Exposure. The Specimen Arrangement in Each Heater is Shown in Figure 9

4.1.2 Results of the 16-Week Exposure Time

After 16 weeks of exposure, all U-bend specimens exposed to $43\ \text{°C}$ [$109\ \text{°F}$] showed an increase buildup of corrosion products compared to those examined at 4 weeks of exposure. Signs of corrosion damage were noted in most of the specimens at the U-bend legs as well as at the crevice between the U-bend and the ceramic shoulder washers. For the double specimens, crevice corrosion developed at the U-bend legs between the inner and outer specimens. Interestingly, the surface appearance of a few 304 and 304L unwelded single U-bend specimens featured corrosion in the form of small striations across the specimen width (Figure 24a). No striation marks were recorded for any of the 316L specimens. To investigate such corrosion features and the presence of cracking, a 304 and 304L single U-bend specimen, which were scheduled to be examined later, were removed from heater 16. Interestingly, none of the 316L specimens showed the presence of cracks.

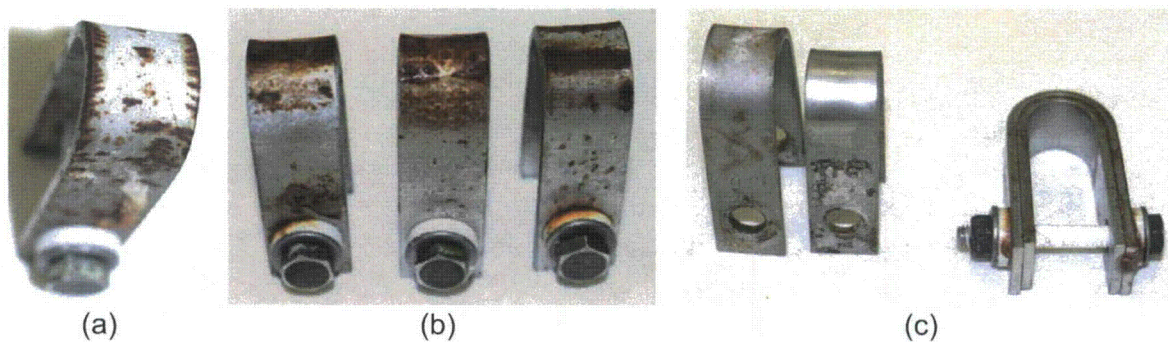


Figure 24 Pictures of (a) a 43 °C [109 °F] 304L U-Bend Specimen Showing Corrosion Product and Striation Marks on the Surface, (b) Corrosion Distress of the 304 Weld U-Bend Specimens, and (c) a 304 Double U-Bend Specimen After 16 Weeks of Exposure

Optical examinations of all the 304 and 304L specimens at 50X magnification revealed the presence of cracks with crack openings roughly of 3 to 5 μm wide. This damage was not discernable at lower magnifications. Extensive cracking was also noted on the double 304 U-bend specimens near the bend apex at the interface between the inner and outer U-bends. To better characterize the type of cracking in the 304 and 304L U-bend specimens, selected single U-bends were cross-sectioned, and the area directly exposed to the environment was polished down to a 1 μm surface finish and electrolytically etched using an oxalic acid with hydrochloric acid solution. Figure 25 shows the cross section appearance at the specimen arch of the 304 and 304L single U-bends. The results showed that cracking was mainly transgranular, but there were regions where the cracks transitioned to intergranular with crack branching, consistent with previous results found for SCC of austenitic stainless steel in chloride environments.

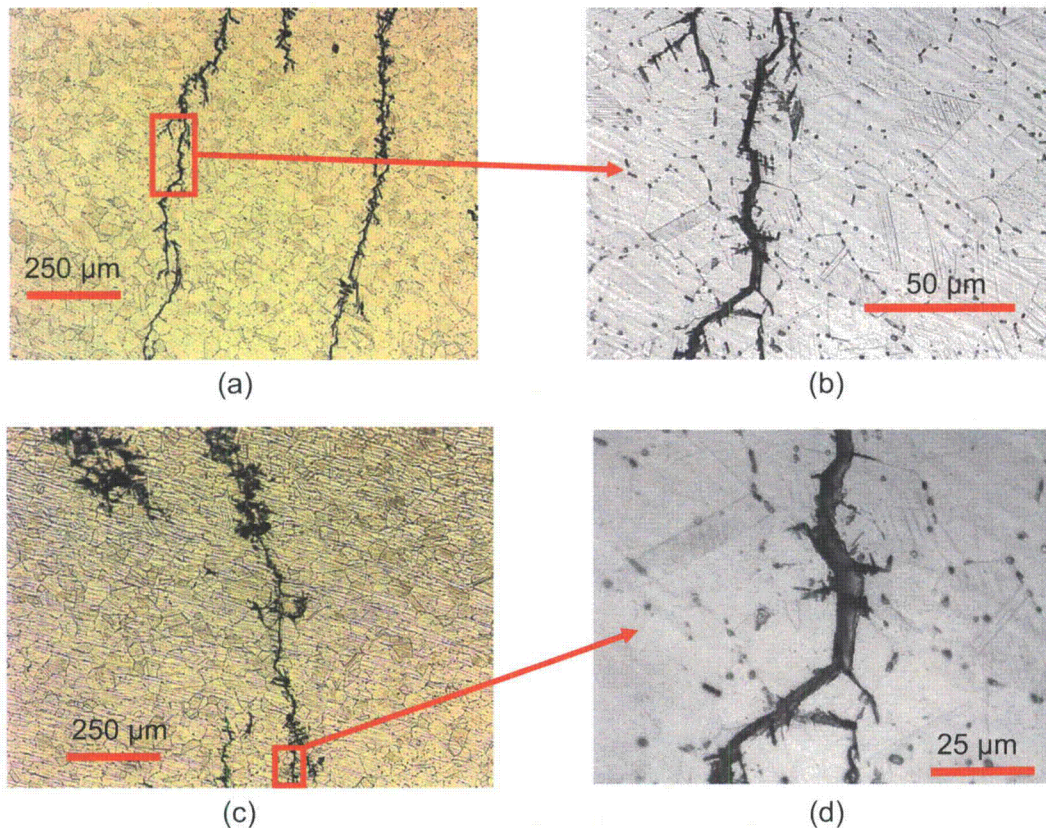


Figure 25 Pictures of SCC Observed Near the Outer Surface at the Specimen Arch: (a and b) a 304 Single U-Bend Specimen and (c and d) a 304L Single U-Bend Specimen. Both Samples Were Exposed to 43 °C [109 °F] for 16 Weeks of Exposure

4.1.3 Results of the 32-Week Exposure Time

For the 32-week exposure, all the single and double welded U-bend specimens showed increasing buildup of corrosion deposits and pit density when compared to previous exposure periods. During this period, cracks were visible by the naked eye on some of the 304 and 304L single U-bend specimens after cleaning (Figures 26 and 27). On the other hand, for the 316L single and double U-bend specimens, optical examination revealed the presence of small cracks (Figure 28). As mentioned earlier, cracking events took place at the apex of curvature around the heat-affected zone for the weld specimens. For all the welded specimens, no cracking was observed in the weld area. For the double specimens, corrosion damage and cracking was more prominent in the outer specimen. SCC in the inner specimen was limited around the edge of the specimen.

To assess the severity of the cracks, selected 304, 304L, and 316L welded and unwelded single U-bend specimens were chosen for microstructure evaluation. The specimens were transversely cut at the bend area and cut again in the longitudinal direction to expose fresh cross section area (Figure 29). Then, the cut samples were mounted in an epoxy, polished to a

600-grit surface finish, and optically examined at a 50X magnification or higher. Figures 30 to 33 show that in all cases the cracks propagated from the outside diameter inwards, covering in some cases the entire specimen thickness. The cracking density was noticeably larger than in previous exposure periods suggesting that the environment was aggressive enough to promote (and propagate) the formation of SCC. As mentioned earlier, cracking appears to be a mixed mode of transgranular and intergranular cracking for all cases, having characteristic branching. However, cracks in the 316L specimens appeared to be much narrower compared to the type 304 and 304L cracks.



Figure 26 Pictures of a Cleaned 304 Stainless Steel U-Bend Specimen Exposed for 32 Weeks at a Temperature of 43 °C [109 °F]

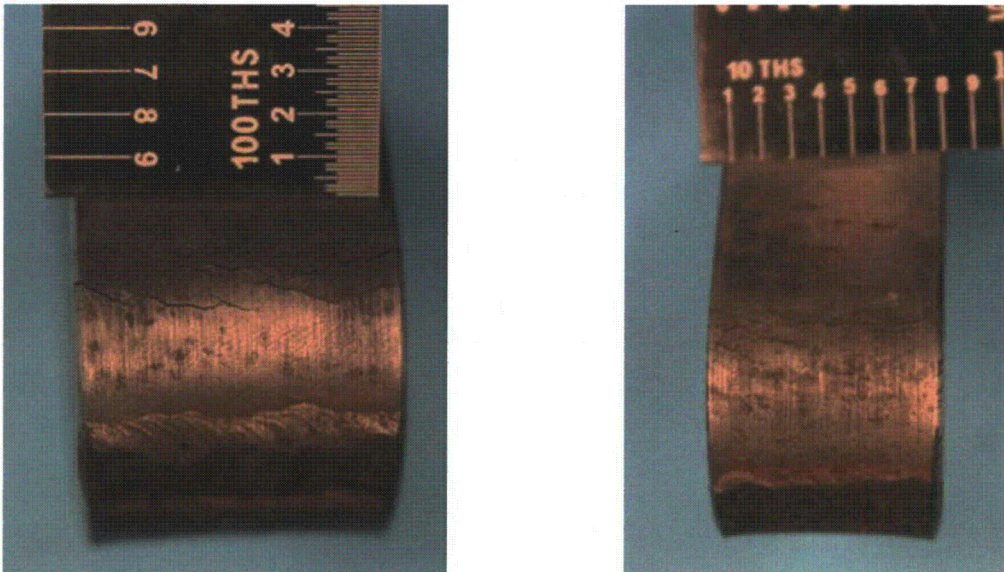
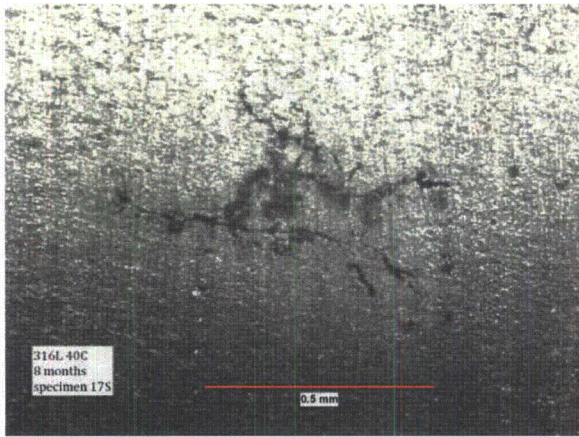


Figure 27 Pictures of a Cleaned 304L Stainless Steel U-Bend Specimen Exposed for 32 Weeks at a Temperature of 43 °C [109 °F]



(a)



(b)

Figure 28 Stereomicroscopic Images of a 316L Stainless Steel: (a) Single and (b) Welded U-Bend Specimens



Figure 29 Pictures of Cut Stainless Steel U-Bend Specimens for Microstructure Evaluation

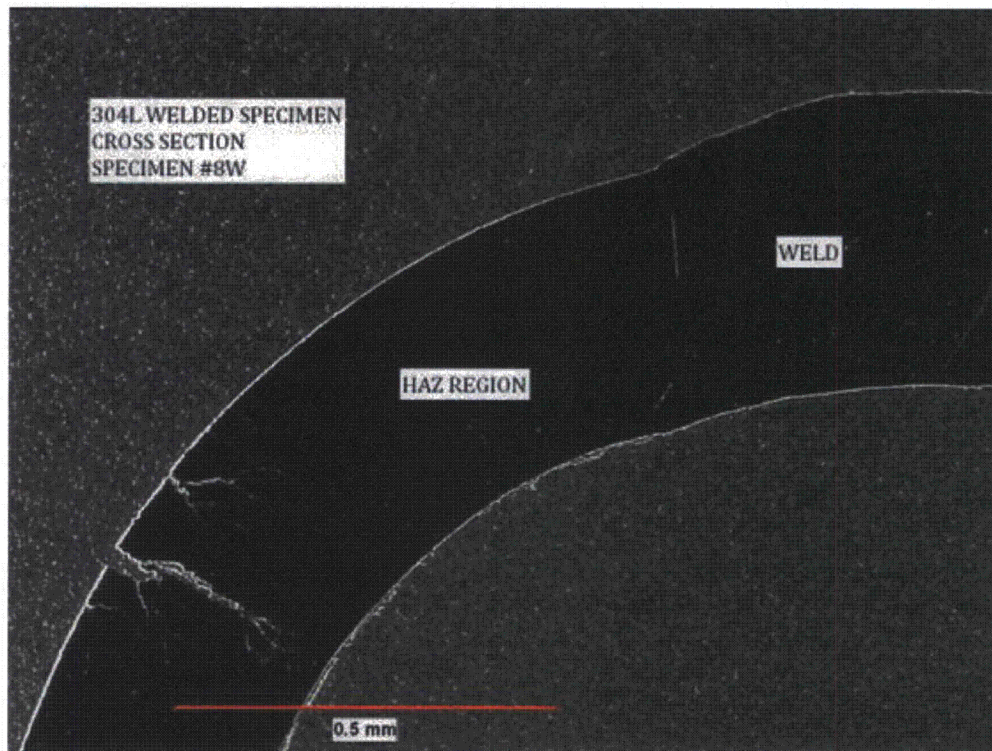


Figure 30 Stereomicroscopic Image of the Cut 304L Weld U-Bend

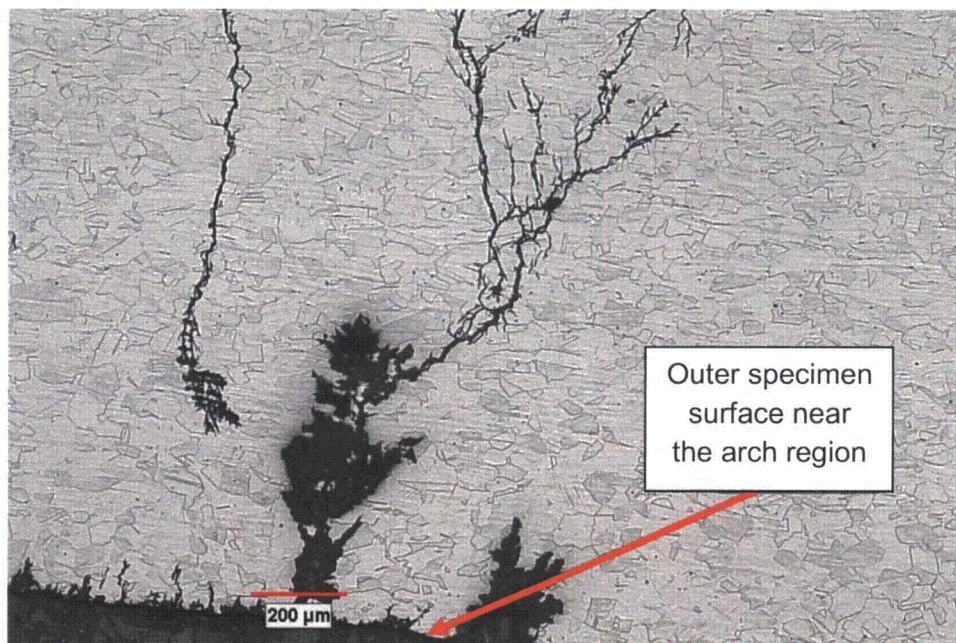


Figure 31 Stereomicroscopic Image of a Cleaned 316L Weld U-Bend Exposed for 32 Weeks at a Temperature of 43 °C [109 °F]

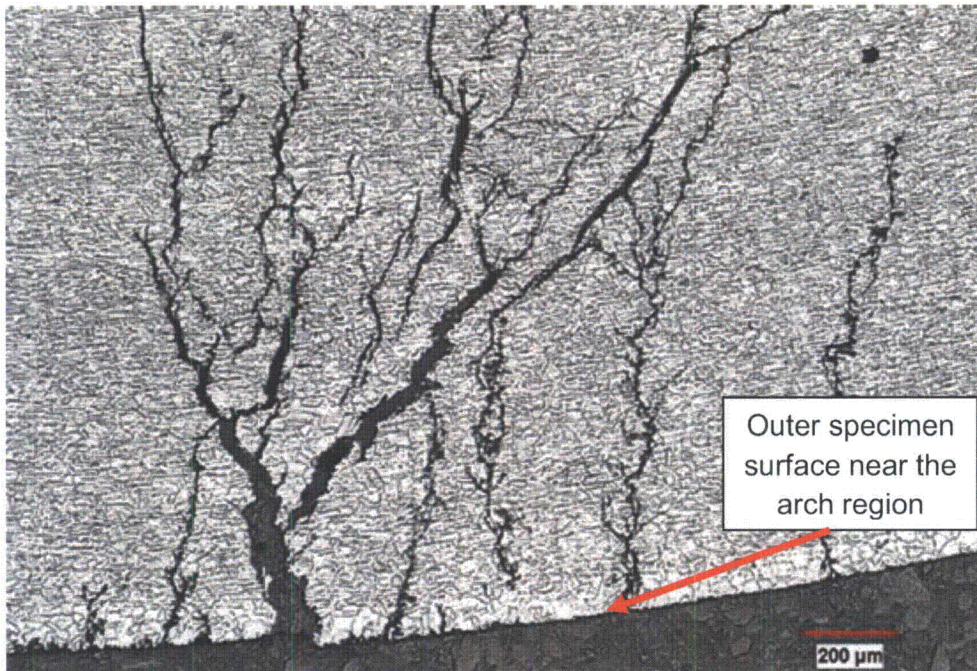


Figure 32 Stereomicroscopic Image of a Cleaned 304L Weld U-Bend Exposed for 32 Weeks at a Temperature of 43 °C [109 °F]

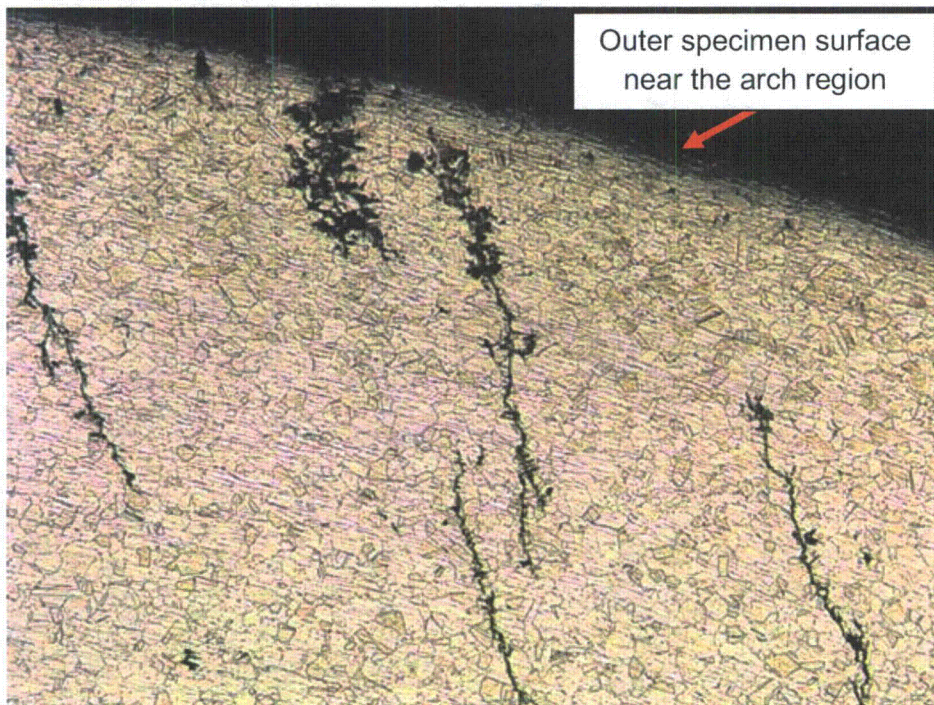


Figure 33 Stereomicroscopic Image of a Cleaned 304 Unwelded Single U-Bend Exposed for 32 Weeks at a Temperature of 43 °C [109 °F]

4.1.4 Results of the 52-Week Exposure Time

After 52 weeks of exposure, all the remaining 43 °C [109 °F] U-bend specimens were taken out of the chamber and photographed. Visual observations of the unwelded 304 and 304L specimens denoted the presence of striation marks on the outer surface near the bend apex in the direction of crack propagation (Figure 34). These striation marks can be associated with crack formation and propagation, although further testing is needed to confirm this scenario. In all cases, the striation marks were covered by corrosion products. The striation marks propagated through the entire width for the unwelded 304L specimens, and extended a few millimeters from the specimen edge for the unwelded 304 specimens.

No striation marks were observed for any of the 316L specimens. Corrosion was more prominent in the 304 and 304L materials throughout the apex curvature and to a lesser extent at the specimen legs. The 316L alloy exhibited the least corrosion distress for all the specimen arrangements. Figure 34 shows the typical appearance of the surface of selected single unwelded U-bend specimens. No additional surface or metallographic analyses were carried out since extensive cracking was recorded in all the specimens during the previous specimen exposure period.

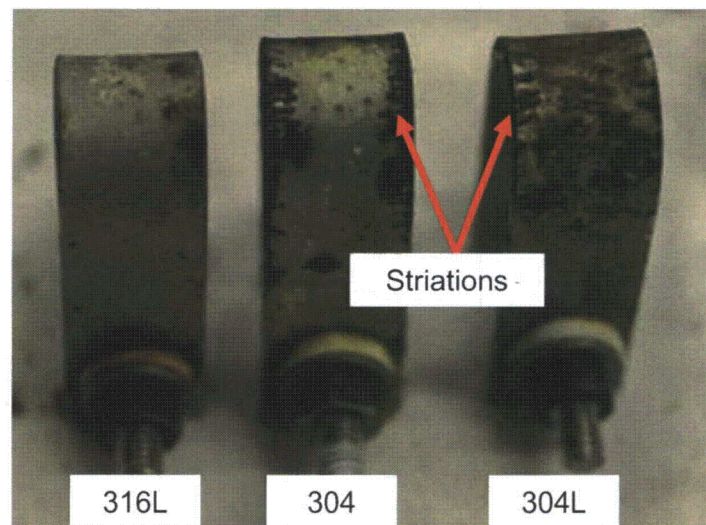


Figure 34 Typical Surface Appearances of Unwelded Single U-Bend Specimens Exposed for 52 Weeks at 43 °C [109 °F]. Striation Marks on the Outer Surface of the 304 and 304L Unwelded Specimens are Indicated

4.2 U-Bend Specimens Held At 85 °C [185 °F] and 120 °C [248 °F]

As can be seen in Figures 35 to 37, all the U-bend specimens exposed to 85 and 120 °C [185 and 248 °F] were covered with a layer of salt deposits. The amount of salt deposited was greatest at the apex of the bend than elsewhere. Visual observations of all the specimens at both temperatures showed that the salt deposits remained dry throughout the exposure time

with no apparent salt deliquescence, even at the high relative humidity values recorded in the chamber. During cleaning, salt deposits were easily washed out from the specimen surface. After 32 weeks of exposure, visual observations of the weld specimens exposed to 85 °C [185 °F] identified the presence of corrosion deposits extending throughout the heat-affected zone. After cleaning, optical examinations revealed evidence of a few isolated pits in a few welded specimens, as illustrated in Figure 38. The pits appeared to be very superficial and located around the specimen within the heat-affected zone. None of the welded and unwelded specimens held at 120 °C [248 °F] exhibited corrosion deposits or pits throughout the entire exposure time. Optical examination at a 500X magnification did not reveal the presence of cracks in all the specimens held at 85 and 120 °C [185 and 248 °F] through the exposure period of 52 weeks.

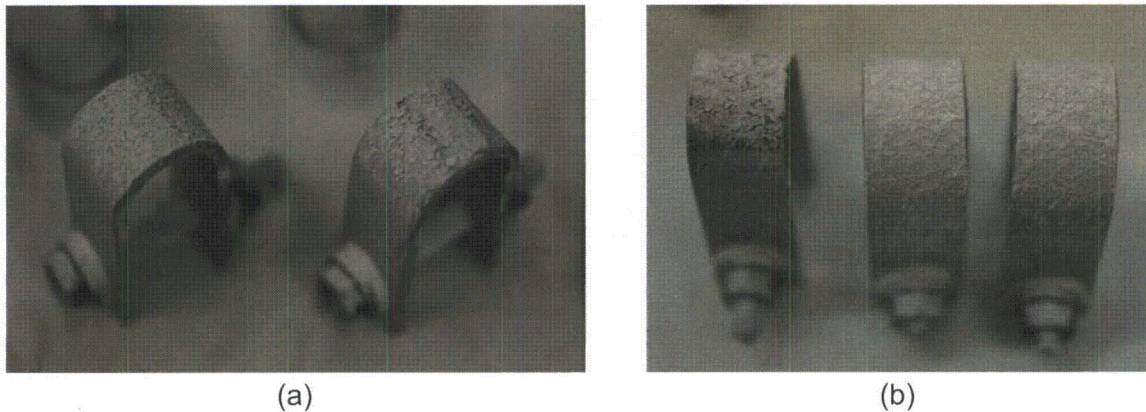


Figure 35 Pictures of the U-Bend Specimens Exposed to (a) 120 °C [248 °F] and (b) 85 °C [185 °F] for 52 Weeks of Exposure

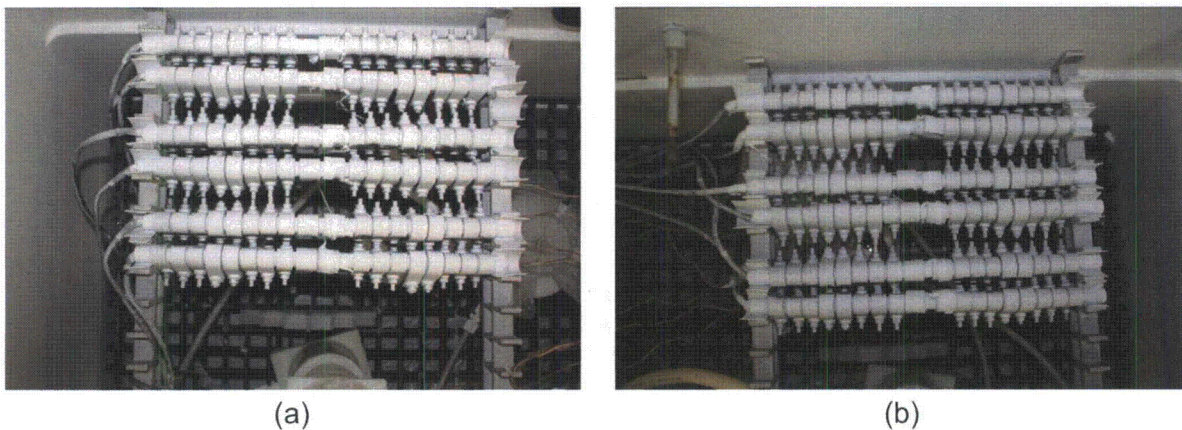


Figure 36 Pictures of the U-Bend Specimens Exposed to (a) 120 °C [248 °F] and (b) 85 °C [185 °F] for 4 Weeks

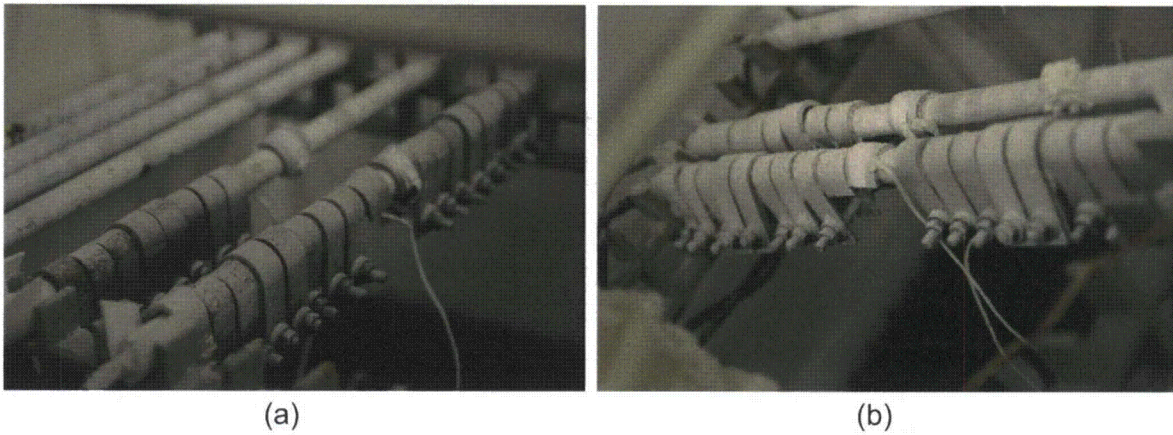


Figure 37 Pictures of the U-Bend Specimens (a) 120 °C [248 °F] and (b) 85 °C [185 °F] Before Removal from the Environmental Chamber After 52 Weeks

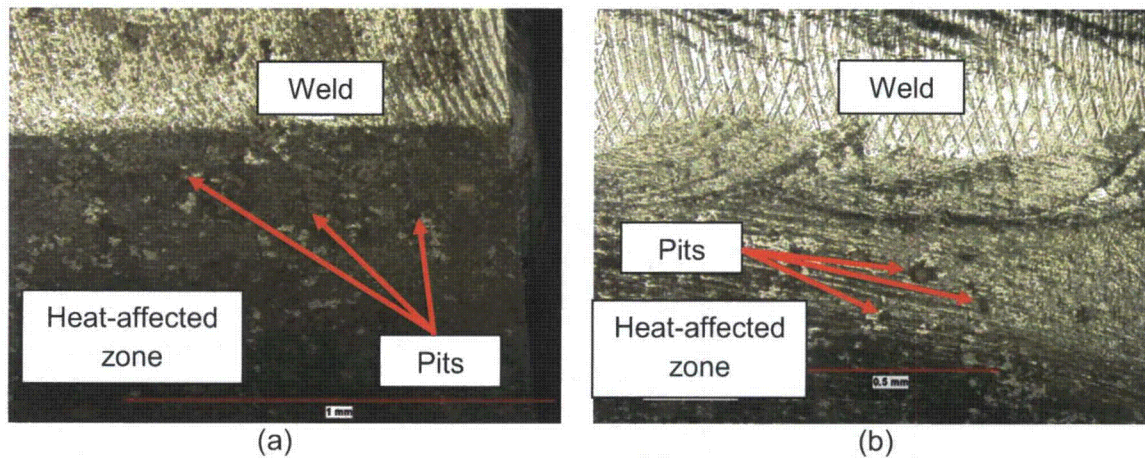


Figure 38 Optical Examinations of the Weld/Heat-Affected Zone of (a) a 304 U-Bend Specimen and (b) a 316L U-Bend Specimen. Both Specimens Were Exposed to 85 °C [185 °F] for 32 Weeks

4.3 Salt Chemical Composition and Deposition Rates

Tables 5 to 8 summarize the chemical analyses carried out on a fraction of the deposited salt collected from the surface of randomly selected 85 and 120 °C [185 and 248 °F] U-bends³ exposed to the salt fog test for 16 weeks. Tables 5 and 6 give the total concentration of anions and cations present in the deposited salt on the 85 and 120 °C [185 and 248 °F] specimens, respectively. The results showed that the species concentrations for the salts from both

³ While salt was visible on the 43 °C [109 °F] U-bends, the significant amounts of corrosion products accumulated on those specimens contaminated the salt extracted so no chemical analyses were conducted.

specimen temperatures were comparable, and that the major constituents were sodium and chloride, making up roughly 68 percent of the simulated sea salt by weight. Moderate concentrations of sulfate, magnesium, calcium, sulfur, and potassium and traces of bromide were also measured for both salts. Tables 7 and 8 show the anion and cations concentrations normalized with respect to the chloride and sodium concentrations, respectively. The results showed that the composition for both the deposited salt and the bulk ASTM sea salt are comparable.

Table 5 Chemical Analyses of a Salt Portion Collected from the Surface of Selected 85 °C [185 °F] U-Bend Specimens

Chemical Species	Concentration
Chloride	0.013 mol/L [469 mg/L]
Sulfate	$7.53 \cdot 10^{-4}$ mol/L [72.3 mg/L]
Bromide	$2.44 \cdot 10^{-5}$ mol/L [2.32 mg/L]
Sodium	297,000 mg/Kg [4.75 oz/lb]
Magnesium	39,300 mg/Kg [0.63 oz/lb]
Sulfur	26,900 mg/Kg [0.43 oz/lb]
Calcium	13,500 mg/Kg [0.22 oz/lb]
Potassium	11,700 mg/Kg [0.19 oz/lb]

Table 6 Chemical Analyses of a Salt Portion Collected from the Surface of Selected 120 °C [248 °F] U-Bend Specimens

Chemical Species	Concentration
Chloride	0.013 mol/L [467 mg/L]
Sulfate	$7.60 \cdot 10^{-4}$ mol/L [73.0 mg/L]
Bromide	$1.75 \cdot 10^{-5}$ mol/L [1.66 mg/L]
Sodium	303,000 mg/Kg [4.85 oz/lb]
Magnesium	39,500 mg/Kg [0.63 oz/lb]
Sulfur	26,900 mg/Kg [0.43 oz/lb]
Calcium	13,800 mg/Kg [0.22 oz/lb]
Potassium	11,900 mg/Kg [0.19 oz/lb]

Table 7 Ratio of Anion Concentration to Chloride Concentration of the Deposited Salt and the Bulk ASTM Sea Salt

Samples	Chloride/Chloride	Sulfate/Chloride	Bromide/ Chloride
Bulk ASTM Sea Salt	1	0.1579	0.0039
Salt on 85 °C [185 °F] U-bends	1	0.1542	0.0049
Salt on 120 °C [248 °F] U-bends	1	0.1563	0.0036

Table 8 Ratio of Cation Concentration to Sodium Concentration of the Deposited Salt and the Bulk ASTM Sea Salt

Samples	Sodium/ Sodium	Magnesium/ Sodium	Sulfur/ Sodium	Calcium/ Sodium	Potassium/ Sodium
Bulk ASTM Sea Salt	1	0.1282	0.0892	0.0405	0.0384
Salt on 85 °C [185 °F] U-bends	1	0.1323	0.0906	0.0455	0.0394
Salt on 120 °C [185 °F] U-bends	1	0.1304	0.0888	0.0455	0.0393

The weight change and the computed salt deposition rates obtained from duplicate flat specimens during the 2-week salt deposition phase of the salt fog test are shown in Table 9. For the 43 °C [109 °F] specimens, a fraction of the weight change was associated with the formation of corrosion products present throughout the specimen surface so the salt deposition rate computations were not solely represented by salt deposits.

Table 9 Salt Deposit Results for the Flat Specimens After a 2-Week Exposure

Temperature, °C [°F]	Salt Weight, mg [oz]	Salt Deposition Rate, mg m ⁻² day ⁻¹ [oz ft ⁻² day ⁻¹]
43 [109]	58.3 [2.06 10 ⁻³]	3,225* [1.06 10 ⁻²]
	57.6 [2.03 10 ⁻³]	3,190* [1.05 10 ⁻²]
85 [185]	36.0 [1.27 10 ⁻³]	1,990 [6.52 10 ⁻³]
	36.3 [1.28 10 ⁻³]	2,010 [6.59 10 ⁻³]
120 [248]	34.6 [1.22 10 ⁻³]	1,915 [6.28 10 ⁻³]
	35.8 [1.26 10 ⁻³]	1,980 [6.49 10 ⁻³]

The specimen area was assumed to be 0.0013 m² [0.014 ft²], based on a single side 5 by 2.5 cm [2 by 1 in] specimen.

* Salt deposition rate computed based on a mixture of deposited salt and corrosion product buildup.

The salt weights and salt deposition rates of the half U-bend samples as a function of time are summarized in Table 10. The deposits on the 43 °C [109 °F] samples consisted mainly of corrosion products so that neither the salt weights nor the salt deposition rates are related only to salt deposition. Conversely, the salt deposition rates of the 85 and 120 °C [185 and 248 °F] samples are expected to be accurate since the weight changes were purely related to salt deposits.

Visual observations of the specimen surface and weight change measurements showed that the deposited salt accumulated over time except for the 120 °C [248 °F] samples exposed to 32 weeks of exposure, which showed a decrease in the amount of accumulated salt. For this case, the decrease in the salt deposit weights can be related to a momentary internal condensation in the chamber, which originated the formation of water droplets that later dripped on the samples, partially removing the salt deposited on those samples. This experimental artifact was corrected such that salt deposition for the 120 °C [248 °F] samples increased again up to the 52-week exposure time. Although this undesired experimental artifact did not allow

the salt deposition rate to be accurately computed for the 120 °C [248 °F] temperature, the condensation did not cause SCC or corrosion damage in the 120 °C [248 °F] samples.

Figure 39 shows the computed salt deposition rates as a function of exposure time. The results showed that the salt deposition rates were largest ($>2,000 \text{ mg m}^{-2} \text{ day}^{-1}$) [$>6.55 \cdot 10^{-3} \text{ oz ft}^{-2} \text{ day}^{-1}$] during the first phase of the salt fog test followed by a sharp decrease during the second phase of the salt fog test, reaching terminal values in the order of $200 \text{ mg m}^{-2} \text{ day}^{-1}$ [$6.55 \cdot 10^{-4} \text{ oz ft}^{-2} \text{ day}^{-1}$] after 112 days. The terminal salt deposition rates are consistent with the measured atmospheric salt deposition rates in the field, recorded at a distance of 100 m [328 ft] from the ocean (Feliu et al., 1999).

Table 10 Salt Deposit Results for the Half U-Bend Samples During the Salt Fog Test

Temperature, °C [°F]	Salt Weight, mg			
	t=28 days (4 weeks)	t=112 days (16 weeks)	t=224 days (32 weeks)	t=364 days (52 weeks)
43 [109]	67.4011*	105.8200*	188.1100*	NA
85 [185]	35.9671	45.1100	87.0480	115.4595
120 [248]	45.8406	92.1700	56.5201	89.6675

The specimen area was assumed to be 0.0013 m^2 [0.014 ft^2] based on a single side 5 by 2.5 cm [2 by 1 in] specimen.

* Weight change was mainly due to corrosion product formation

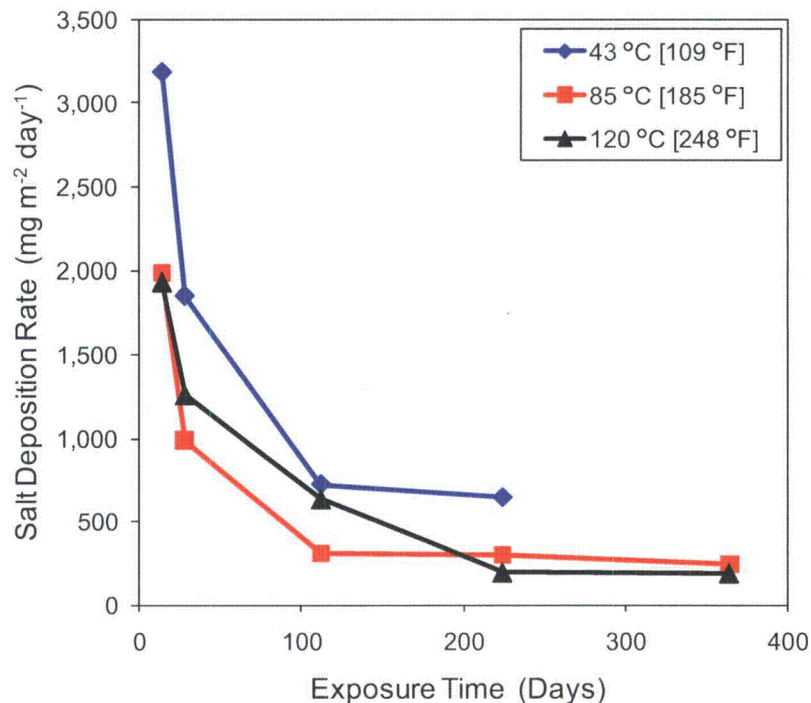


Figure 39 Salt Deposition Rates as a Function of Time for the Half U-Bend Samples Exposed to the Salt Fog. Due to the Condensation Issue Inside the Chamber, the Salt Deposition Rates for the 120 °C [248 °F] Samples are Inaccurate Between 100 and 365 Days of Exposure

4.4 Discussion

The SCC results of the 52-week exposure to sea salt fog and the intermediate exposure periods are shown in Figures 40 to 42 for all of the materials and temperatures examined. The results showed that at or above roughly 85 °C [185 °F], the 304, 304L, and 316L austenitic stainless steels did not develop SCC, despite the minor corrosion damage noted for the specimens held at 85 °C [185 °F].

According to several research studies (Truman, 1977; Ford and Silverman, 1980), while higher temperatures can typically lead to an increased probability of SCC, the results presented here seem to be contradictory. This contradicting behavior can be explained by the deliquescent nature of the deposited salt as a function of the specimen temperature (described in detail in Section 5). Although the chamber relative humidity during the salt fog test temporarily reached around 75 percent, at temperatures of the specimens higher than 85 °C [185 °F], the relative humidity close to the heated specimen surface attained a maximum value of 18 percent. This relative humidity value falls below the deliquescence point for both sodium and magnesium chlorides present in the deposited salt. Thus, the salt deposited on the higher temperature U-bend specimens did not deliquesce throughout the test exposure, preventing both SCC initiation and formation of corrosion products. For the specimens maintained at 43 °C [109 °F], however, the relative humidity near the specimen surface briefly reached ~75 percent, which is above the deliquescence point for sodium chloride. As a result, the salt deposited on the specimens started to deliquesce, promoting SCC initiation as well as formation of corrosion products.

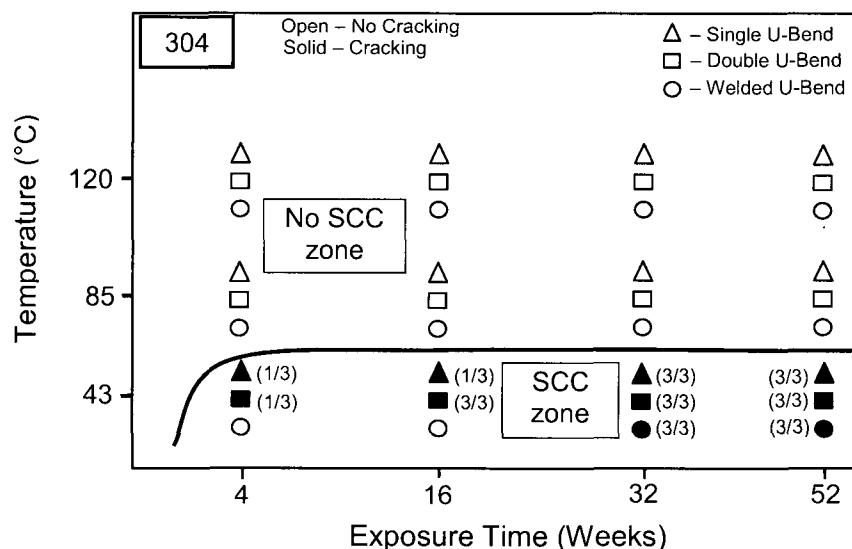


Figure 40 SCC Susceptibility Map for the Type 304 Stainless Steel (Number in Parenthesis States Number of Specimens Cracked/Total Number of Specimens Tested)

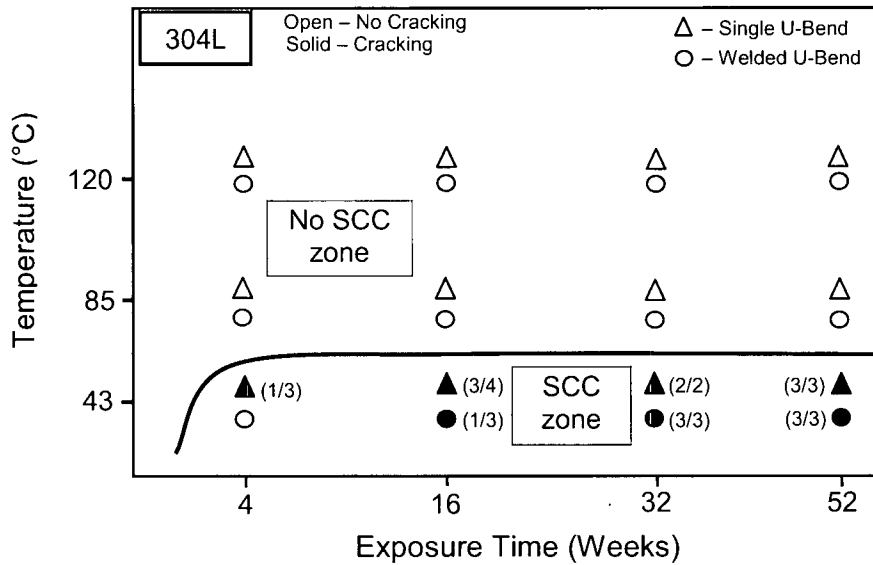


Figure 41 SCC Susceptibility Map for the Type 304L Stainless Steel (Number in Parenthesis States Number of Specimens Cracked/Total Number of Specimens Tested)

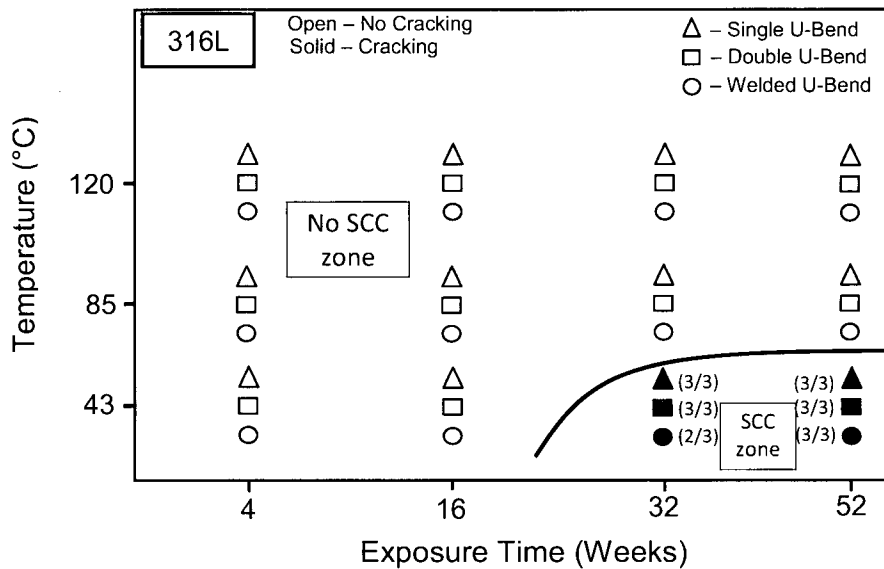


Figure 42 SCC Susceptibility Map for the Type 316L Stainless Steel (Number in Parenthesis States Number of Specimens Cracked/Total Number of Specimens Tested)

Comparing the results in Figures 40 through 42, there is a perceptible difference in the SCC susceptibility of the various material types tested. Both the 304 and 304L stainless steel materials showed evidence of SCC at 4 weeks of exposure and SCC was more conspicuous as exposure time increased. However, cracking of the 316L stainless steel did not occur until after

32 weeks of exposure. This suggests, as expected, that the composition of the material plays a role in the SCC susceptibility.

Both welded and unwelded single and double 304, 304L, and 316L stainless steels exposed to 43 °C [109 °F] exhibited corrosion degradation, in the form of pits and macro corrosion to some extent. This type of corrosion attack was more noticeable around the specimen apex curvature where the weld for the welded specimens was located. Nevertheless, the dominant pit initiation, crack formation and propagation mechanisms are unclear based on the information obtained from this study. Literature information (Wranglen, 1974; Sudesh et al., 2007) suggests that pit nucleation of unwelded stainless steels exposed to chloride containing solutions occurs mainly at or near manganese sulfide and mixed oxide/sulfide inclusions present at the stainless steel surface. The dominant pit nucleation mechanisms are attributed to the local decrease in pH resulting from inclusion dissolution and chromium depletion surrounding the inclusions.

For the welded stainless steels, the most common and relevant factors affecting pit initiation are related to the interdendritic attack in weld metal zone and sensitized grain boundaries in the heat-affected zone, resulting in localized chromium dissolution of the passive layer. The dissolution of chromium is typically greater at and around the heat-affected zone for the weld specimens especially for the type 304 stainless steels where chromium carbides can precipitate at the grain boundaries during welding by a process called sensitization (Tsai and Eagar, 1984). This mechanism explains the accelerated corrosion damage at the heat-affected zone for the weld specimens. It should be noted that the proposed scenario described above may not be required for SCC or enhanced corrosion of weldments because brittle phase formation in the heat-affected zone can also promote SCC as well as general and localized corrosion.

The evaluation of crevice corrosion on the double U-bend specimens showed that crevices did not appear to be overly prejudicial as corrosion was limited to the specimen edges with minimal corrosion degradation inside the crevice. This observation can be associated with the limited access of salt deposited inside the crevice.

As mentioned earlier, cracking events and pitting corrosion recorded in all the 43 °C [109 °F] specimens were concentrated within the arch area of the 304, 304L, and 316L specimens, where the tensile stresses were greatest, and at the heat-affected zone for the welded specimens. Visual examination results suggest that cracks started at or near the pits, where residual stresses were also expected to be significant, and propagated through the specimen cross section. This observation is consistent with previous studies (Szklańska-Smiałowska and Gust, 1979; Turnbull et al., 2009). In addition, microscopic evidence suggests that the cracking events were mainly transgranular with sections of intergranular branching morphology, in agreement with the results reported elsewhere (Garcia et al., 2008; Guerre et al., 2005).

An evaluation of the environment in the test chamber during the highest relative humidity cycle was examined to understand the conditions that led to the SCC of the U-bend specimens. The trends of relative humidity versus temperature for various absolute humidity values are shown in

Figure 43. This figure states that the salt deposited on the 43 °C [109 °F] specimens would have absorbed moisture from the environment because the relative humidity increased above both the magnesium chloride and the sodium chloride deliquescence threshold. As a result, SCC was likely to initiate if the remaining conditions for SCC development were met. However, no moisture would have been expected to absorb in the salt deposited on the 85 and 120 °C [185 and 248 °F] U-bend specimens because the relative humidity around these salts was always below the deliquescence point for both sodium chloride and magnesium chloride. As a result, no SCC was noted in any of the specimens held at or above 85 °C [185 °F]. Even though there was plenty of salt on the surface of these materials, the surrounding air was too dry and did not allow for the deliquescence of salt, which is necessary for SCC to occur.

The work by Prosek et al. (2009) indicated that the 304 stainless steel did not crack in sodium chloride at 40 °C [104 °F] and a relative humidity of 70, 50, or 30 percent after 10 weeks exposure. This observation is likely related to the fact that each of the environmental conditions tested by Prosek was constant throughout the exposure period and could have led to a partial deliquescence of sodium chloride. As indicated in the work by Fairweather et al. (2008), a substantial variation in SCC behavior can be observed with varying relative humidity in chloride containing media at 60 °C [140 °F]. Usually, there is a critical relative humidity (~60 percent) that SCC is most severe. As can be seen in Figure 43, the 43 °C [109 °F] U-bend specimens were cycled between a high and low relative humidity condition so that they were repeatedly exposed to this critical SCC environment. While this humidity cycle in the environmental chamber appeared to be extreme, it is similar to the diurnal weather variations in relative humidity and temperature at many storage cask locations.

The results obtained from this investigation are likely to be conservative with respect to the actual conditions observed in a dry storage cask placed inside a concrete bunker. The environmental conditions inside the bunker are likely to be different from those outside the bunker, even though natural ventilation is being employed. Secondly, the measured maximum absolute humidity achieved during the salt fog test was $\sim 60 \text{ g/m}^3$ [$\sim 2.17 \cdot 10^{-6} \text{ lb/in}^3$]. Reported environmental data from around the U.S. coast suggests that the maximum absolute humidity values are in the order of 30 g/m^3 [$1.08 \cdot 10^{-6} \text{ lb/in}^3$], (NOAA, 2010). With a lower absolute humidity, the relative humidity near the specimens would have been lower and deliquescence of the deposited salt may not have taken place. While these tests may have been conservative, the results are important because they suggest that the deliquescence of dry deposited sea salt can lead to SCC of austenitic stainless steels when the cask temperature is slightly above the ambient temperature.

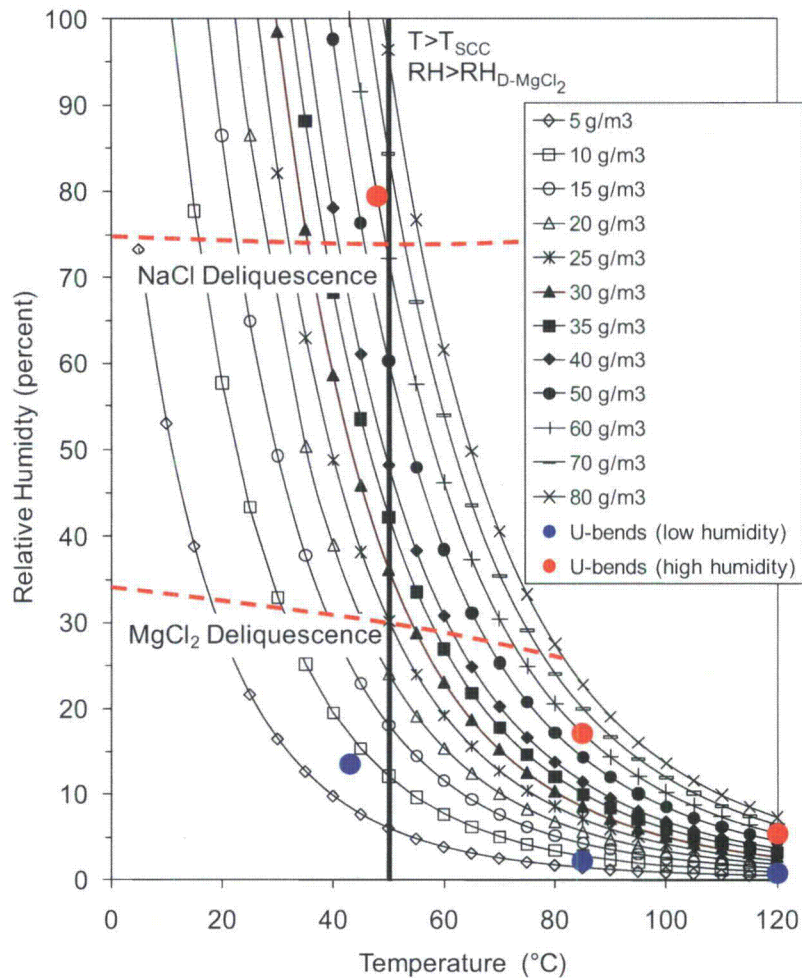


Figure 43 Evolution of the Relative Humidity as a Function of Temperature Computed for Various Absolute Humidity Values. The Region Between the Red (Maximum Humidity) and Blue (Minimum Humidity) Symbols Indicate the Expected Environmental Conditions Near the U-Bend Surface in the Salt Fog Test

4.5 Implications of the Results

As mentioned earlier, initiation of SCC requires three important criteria, including high enough stresses, a susceptible material, and a detrimental environment. The laboratory testing conducted in this investigation had all three requirements and demonstrated that SCC can effectively occur within 32 weeks of exposure in 304, 304L, and 316L stainless steels (such as those used for dry storage cask) maintained at temperatures around 43 °C [109 °F] and at an absolute humidity of 60 g/m³ [2.16 10⁻⁶ lb/in³]. Based on the results of this investigation, estimation of the SCC acceleration factor used in the laboratory testing and its implications on durability and SCC development to actual dry storage cask units in the field are difficult to compute and requires various assumptions to be made, as described next.

One of these assumptions is related to the differences in the stress levels found on a dry storage cask compared to those used in the U-bend samples. The U-bend samples have typical stress levels in excess of the material yield stress, which is likely higher than those observed for an actual dry storage cask. Therefore, to compare the laboratory tests to the field conditions, it is necessary to assume that the dry storage cask material will behave similar to the U-bend samples.

The second assumption relates to the environment surrounding the dry cask. The laboratory U-bend samples had salt deposited cyclically on the surface during the entire test. For field applications, it is not clear at this time whether salt can ingress the concrete vault through the passive ventilation system and deposit on the outer cask metal surface. In addition to salt reaching the dry storage cask, it is not well understood the amount of salt needed to initiate SCC. On a first approximation, the SCC initiation processes will not likely start until enough salt is present at the metal surface, which may take months to years depending upon the salt deposition rate. Comparing the salt deposition rates between the laboratory test and atmospheric environments, it can be concluded that for the first two weeks of exposure, laboratory salt deposition rates are approximately equivalent to 5 to 18 months of accumulated salt deposition (assuming a deposition rate of 200 to 50 mg m⁻² day⁻¹, respectively, at a distance of 100 m [328 ft] from the ocean). Actual deposition rates are dependent on a number of factors, including wind velocity and direction, humidity, and topography.

The next unknown environmental parameter surrounding the dry cask is the absolute humidity. As shown in the results of this work, the absolute humidity must be high enough so that the relative humidity at the surface of the dry storage cask will lead to the deliquescence of the deposited salt. In this investigation, the absolute humidity was temporarily increased to 60 g/m³ [2.16 10⁻⁶ lb/in³] in order to achieve the target relative humidity of 70 percent (necessary to deliquesce sodium chloride). However, this absolute humidity value is not likely to be achieved under normal atmospheric conditions. With a typical maximum absolute humidity of 30 g/m³ [1.08 10⁻⁶ lb/in³], deliquescence of sodium chloride could occur at temperatures below 36 °C [97 °F], which may be too low for SCC to initiate. However, as shown in the experimental tests, the sea salt deposited on the surface of the samples contained magnesium chloride in addition to sodium chloride. The deliquescence point of magnesium chloride is at a relative humidity of roughly 30 percent, and magnesium chloride can induce SCC initiation in stainless steels. Deliquescence of magnesium chloride in an environment with an absolute humidity of 30 g/m³ [1.08 10⁻⁶ lb/in³] can occur at temperatures up to 54 °C [129 °F], which is definitely in the range of SCC to develop. With this understanding, the question remains as to what relative humidity is necessary for SCC to occur with a deposited salt mixture of mainly sodium chloride, but with some magnesium chloride. However, in order to compare the data of this test to actual field conditions, it is necessary to make the conservative assumption that the relative humidity must be over 30 percent for SCC development.

With all of these assumptions being made, the last issue that must be discussed is the actual environment where the dry storage cask is placed. Reviewing the data from NOAA

(NOAA, 2010), it can be seen that not all locations along the coastline are the same. Moreover, the environmental conditions vary from location to location. Secondly, there will also be a seasonal variation in the environmental conditions. As demonstrated in this investigation, the outer temperature of the dry storage cask will modify the relative humidity on the surface of the dry storage cask, thereby affecting the deliquescence of the salt deposited on the surface. The outer surface temperature of the dry cask storage will vary from cask to cask depending upon the type of cask, used fuel, and operational history. Therefore, it is necessary to know the environmental and cask conditions to determine how the experimental results will compare to the dry cask storage in the field.

However, the laboratory and field data can be compared if the assumption is made that each day the environment surrounding the dry storage cask follows one wet and dry cycle, i.e. the relative humidity cycles around 30 percent. Under this situation, then the field condition can be compared to the laboratory tests, which had four wet and dry cycles per day. Then, the time to SCC initiation would be expected to be roughly between 32 and 128 weeks. However, this is still a conservative estimation because it does not take into account the operating history of the dry storage cask and the local environmental properties along with many other assumptions previously discussed.

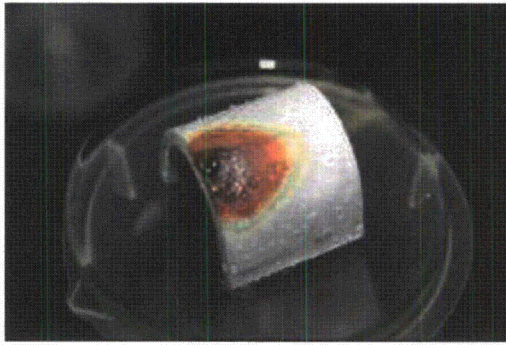
5 SCC COMPLEMENTARY TESTING

5.1 Half U-Bend Specimen Testing

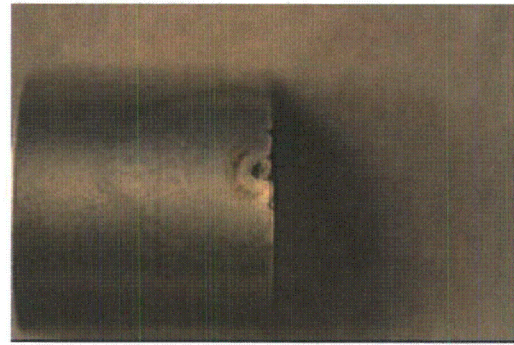
Immediately after exposure periods of up to 2 months, visual observations identified salt deliquescence for the salt-deposited half U-bend samples exposed to 65 °C [149 °F] and 70 percent relative humidity as shown in Figure 44. Concurrently, formation of corrosion products and localized pitting corrosion around the arch outer diameter and near the sample edges began to appear. Laser profilometry measurements (Figure 45) showed that pit depth was roughly 380 μm [0.15 in], indicating that the localized corrosion rates were in the order of 4.5 mm/yr [0.180 in/yr].⁴ Similar observations were made for half U-bend samples with salt deposits exposed to 50 °C [122 °F] and 65 percent relative humidity (Figure 43a). At 50 °C [122 °F] and relative humidity values of 40 and 50 percent (Figures 44a and 45a), the salt-deposited samples showed a salt layer still present on the surface, in addition to corrosion in the form of small isolated pits after a 2-month exposure. Interestingly, no SCC was noted in any of the samples despite the favorable environmental conditions for SCC initiation.

Visual observations of the droplets of simulated sea salt and magnesium chloride placed on half U-bend samples exposed to 50 °C [122 °F] and relative humidity values of 40, 50, and 65 percent showed formation of corrosion deposits and isolated pits after a 2-month exposure (Figures 46 to 48). The samples with simulated sea salt droplets showed some degree of salt crystallization, likely rich in sodium chloride. For the environmental conditions examined, it is speculated that when the simulated sea salt deliquesced, sodium chloride precipitated out of the solution and remained as crystals on the surface of the sample whereas the magnesium chloride initially present in sea salt remained in solution, originating the formation of red rust corrosion. All the samples with sodium chloride droplets showed similar formation of crystals compared to the sea salt droplets, but in this case, the sample remained free of corrosion deposits throughout the entire exposure time. Nevertheless, no SCC formation was recorded in any of the samples with salt droplets.

⁴ The large localized corrosion rates measured in this study cannot be directly related to those in actual casks since the environmental conditions used in the complimentary tests were held constant.



Before cleaning



After cleaning

Figure 44 Typical Surface Appearance Observed for the 304 Stainless Steel Half U-Bend Samples Subjected to 2-Month at 65 °C [149 °F] and 70 Percent Relative Humidity

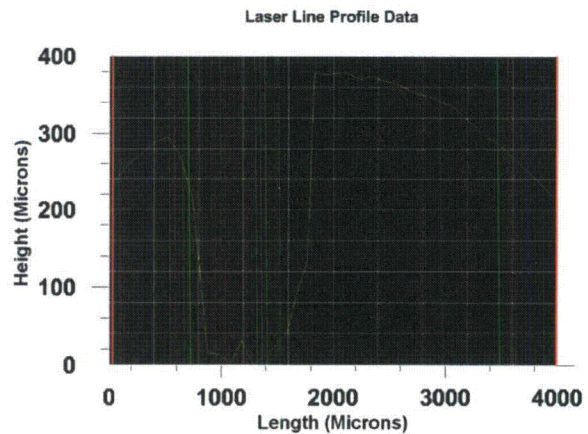
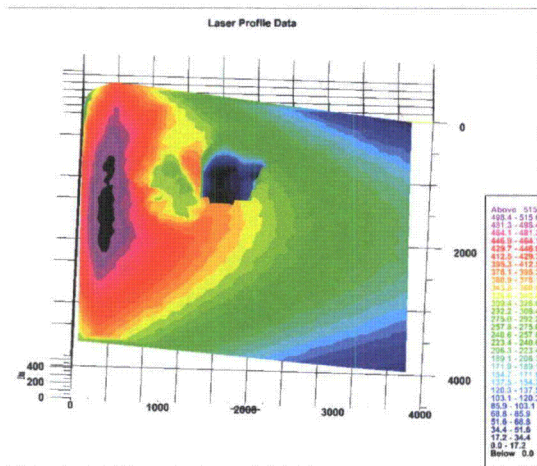
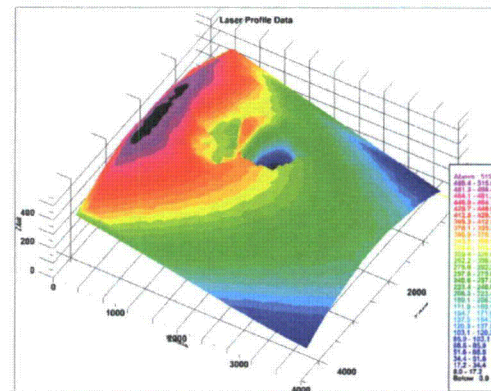
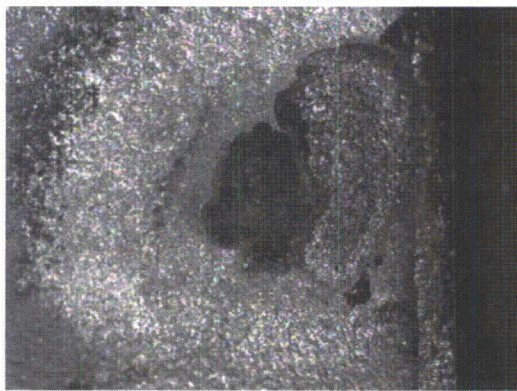


Figure 45 Laser Profilometer Data Evaluating Depth of Pitting on a 304 Stainless Steel Half U-Bend Sample Exposed to 2-Month at 65 °C [149 °F] and 70 Percent Relative Humidity

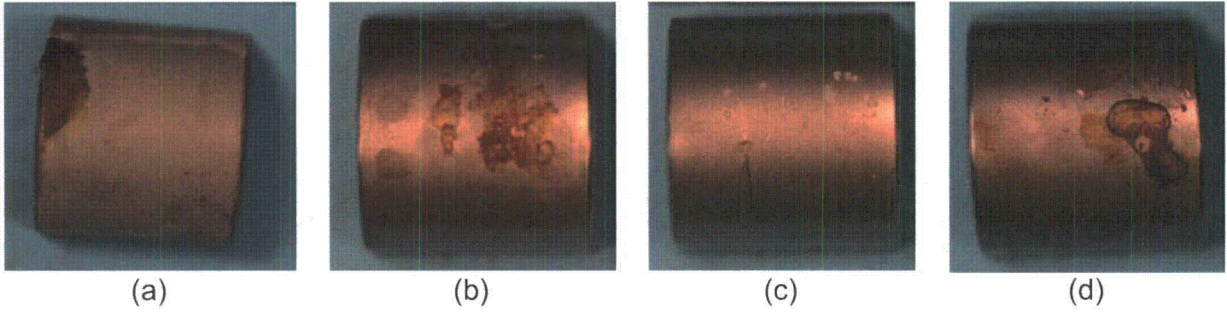


Figure 46 Typical Surface Appearance (Before Cleaning) of the 304 Stainless Steel Half U-Bends Exposed to 50 °C [122 °F] and 65 Percent Relative Humidity for 2 Months:(a) Initial Salt Deposits on the Surface During the Salt Fog Test, (b) Simulated Sea Salt Droplets, (c) Sodium Chloride Droplets, and (d) Magnesium Chloride Droplets

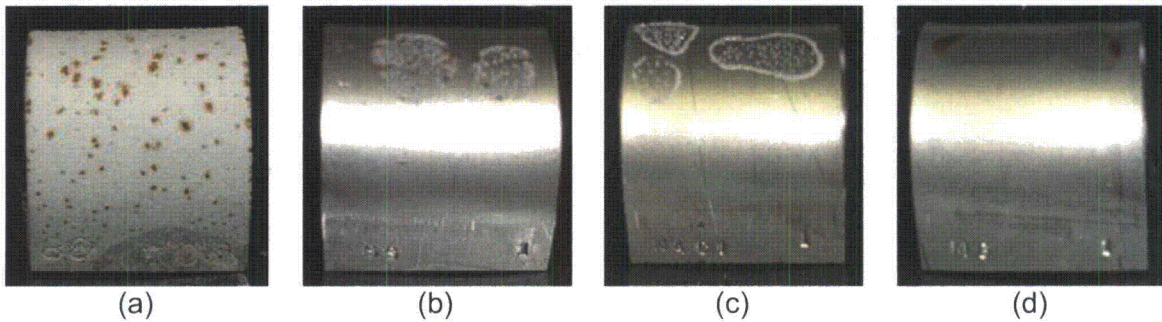


Figure 47 Typical Surface Appearance (Before Cleaning) of the 304 Stainless Steel Half U-Bends Exposed to 50 °C [122 °F] and 40 Percent Relative Humidity for 2 Months:(a) Initial Salt Deposits on the Surface During the Salt Fog Test, (b) Simulated Sea Salt Droplets, (c) Sodium Chloride Droplets, and (d) Magnesium Chloride Droplets

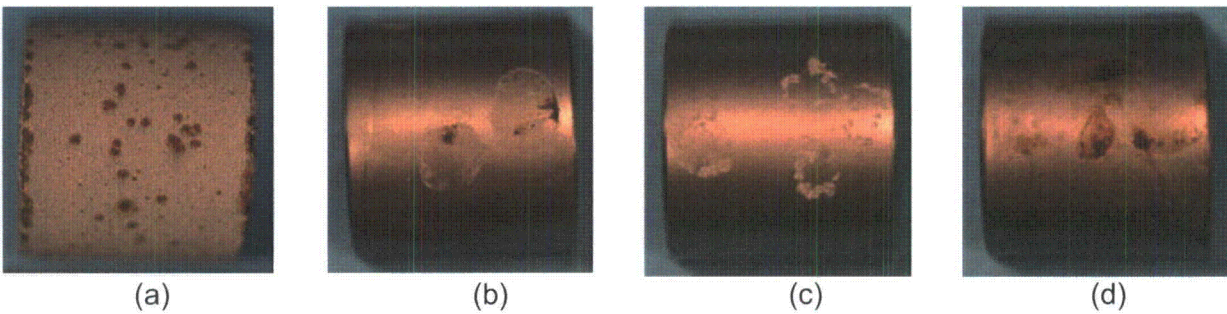


Figure 48 Typical Surface Appearance (Before Cleaning) of the 304 Stainless Steel Half U-Bends Exposed to 50 °C [122 °F] and 50 Percent Relative Humidity for 2 Months:(a) Initial Salt Deposits on the Surface During the Salt Fog Test, (b) Simulated Sea Salt Droplets, (c) Sodium Chloride Droplets, and (d) Magnesium Chloride Droplets

5.2 Salt Deliquescence and Efflorescence

Simulated sea salt, magnesium chloride, sodium chloride, and a sample of Corpus Christi salt were placed in a humidity chamber at 50 °C [122 °F] (Figure 49). Visual examination revealed that at 20 percent relative humidity, all four salts appeared dry. Once the relative humidity was increased to 35 percent, the magnesium chloride salt deliquesced as expected. On the other hand, the simulated sea salt and Corpus Christi salt appeared to absorb water from the environment, causing a light darkening of the salts. Afterwards, no significant changes took place until the relative humidity reached 75 percent, at which point the simulated sea salt, Corpus Christi salt, and sodium chloride deliquesced.

The same test, repeated at 80 °C [176 °F] showed that when the relative humidity was held at 20 percent, all the salt samples were dry. Once the relative humidity increased to 30 percent, the magnesium chloride sample deliquesced. Above 30 percent, the Corpus Christi salt and simulated sea salt appeared to have adsorbed water, but both salts did not deliquesce until the relative humidity reached 70 percent. However, the sodium chloride did not deliquesce until the relative humidity increased to 75 percent. It appears that the increase in temperature may have decreased the relative humidity necessary for deliquescence of the magnesium chloride containing salts, consistent with the results reported in the literature (Racine, 2005).



(a)



(b)



(c)



(d)



(e)



(f)

Figure 49 Deliquescence Experiments Conducted at 50 °C [122 °F] and Relative Humidity of a) 20 Percent, b) 35 Percent, c) 45 Percent, d) 55 Percent, e) 65 Percent, and f) 75 Percent. The Salt Sample Labels are: (A) Corpus Christi Salt, (B) Simulated Sea Salt, (C) Sodium Chloride, and (D) Magnesium Chloride

5.3 Environmental Temperature and Humidity Profiles

The results of the humidity/temperature measurements as a function of the distance from the U-bend surface are shown in Figure 50. The results showed that the temperature recorded at 0.5 cm [0.20 in] from the U-bend surface varied from 47 to 53 °C [117 to 127 °F] for the U-bends temperatures of 60 and 120 °C [140 and 248 °F], respectively. Between 0.5 cm [0.20 in] and 1.7 cm [0.67 in], the temperature for all the cases examined showed an abrupt drop to ~37 °C [~99 °F] and remained nearly constant afterwards reaching an apparent terminal value of ~35 °C [~95 °F], comparable to the chamber bulk temperature. The relative humidity recorded at 0.5 cm [0.20 in] from the U-bend surface varied from 27 to 43 percent for the U-bends temperatures of 60 and 120 °C [140 and 248 °F], respectively. Between 0.5 cm [0.20 in] and 1.7 cm [0.67 in], the relative humidity for all the cases increased rapidly, ranging from 75 percent (for the U-bends maintained at 120 °C [248 °F]) to 88 percent (for the U-bends maintained at 60 °C [140 °F]). Afterwards, the relative humidity showed a gradual increase, reaching values of 82 percent to 95 percent at 5.5 cm [2.16 in] from the U-bend surface. If the relative humidity line were linearly projected to the surface of the U-bend, the relative humidity would be less than 30 percent for all cases, which is near the deliquescence threshold for magnesium chloride. On the other hand, the absolute humidity does not seem to vary significantly with distance for the U-bend surface and drops only a few g/m³ closer to the heated U-bends.

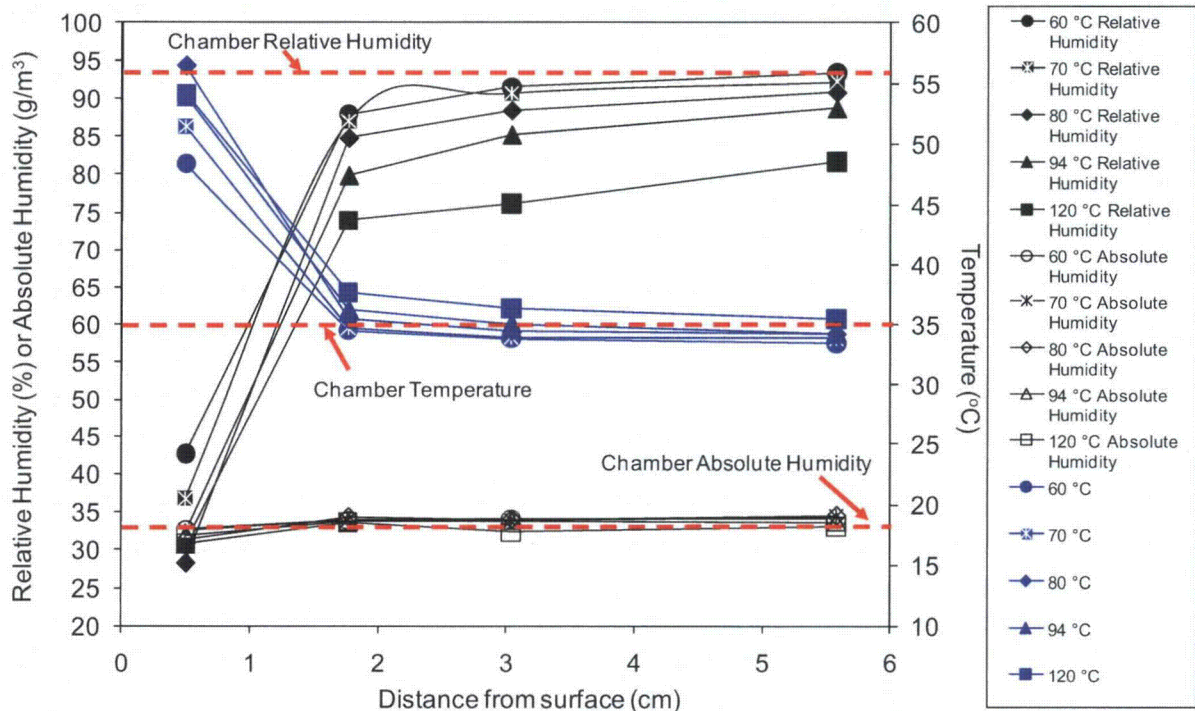


Figure 50 Temperature, Absolute Humidity, and Relative Humidity Profiles as a Function of Distance from the U-Bend Samples Heated at Different Temperatures

5.4 Discussion

Experimental observations showed that no SCC initiated on the half U-bend samples, suggesting that tensile stress levels acting on the samples were not sufficient to promote SCC compared to the full U-bend specimens tested under constant strain. One potential explanation of this observation is that once the metal was stressed during bending, the lack of stressing elements in the half U-bend sample to supply a constant level of strain could have caused substantial residual stress relaxation throughout the metal surface right after bending. This large stress relaxation would ultimately lower the residual stresses in the metal, reducing the probability of SCC development even though the environmental conditions were favorable for SCC initiation.

While the results from the half U-bend samples cannot be used as an indicator for stress corrosion cracking, the half U-bend results are useful in understanding the wetting conditions that could lead to SCC. As indicated above, the half U-bend samples that were held at 50 °C [122 °F] and a relative humidity of 45 percent showed pitting, for all samples except the ones exposed to sodium chloride. This indicates that even though the simulated sea salt mainly consists of sodium chloride, the amount of magnesium chloride in the salt is enough to allow the formation of a chloride solution at 45 percent relative humidity, which is well below the deliquescence point of sodium chloride but above the deliquescence point of magnesium chloride. Therefore, the presence of magnesium chloride in the salt is an important aspect to consider in the deliquescence of sea salt and the initiation and propagation of pitting corrosion and stress corrosion cracking.

As indicated in Figure 50, temperature, relative humidity, and absolute humidity vary with the distance measured from a heated metal. The results obtained in this study showed that the absolute humidity was nearly constant with distance. However, the temperature and relative humidity are strongly dependent on the distance from the heated surface. Experimental observations denoted that the temperature would increase sharply while the relative humidity will drop upon approaching the surface of the heated metal. At 60 to 120 °C [140 to 248 °F], the relative humidity decreased from a bulk value of 95 percent down to approximately 30 percent at the metal surface, when the bulk temperature was held at 35 °C [95 °F]. A relative humidity value of 30 percent is close to the deliquescence point for magnesium chloride. This suggests that for increasing canister temperatures, relative humidity values will decrease and the environmental conditions necessary for SCC would not occur. This is consistent with the results of the salt fog experiments for which observed salt deposits formed on the surface of the 85 and 120 °C [185 and 248 °F] U-bend specimens.

6 CONCLUSIONS

The findings of this investigation are as follows:

- During phase I testing, cyclic simulated sea salt solution was directly sprayed on welded and unwelded U-bend specimens made of 304, 304L, and 316L stainless steels at 25, 93, and 176 °C [77, 200, 350 °F]. Within 2 months of exposure, no cracking was recorded in any of the 25 °C [77 °F] specimens. On the contrary, all the 93 and 176 °C [200 and 350 °F] specimens produced extensive cracking and corrosion degradation primarily, along the leg and arch-to-leg transition of the U-bends. At these elevated temperatures, the water present in the simulated sea salt was expected to have boiled quickly from the specimen surface, leaving behind a dry salt, and thus, preventing SCC formation. However, a significant decrease in temperature during the spray cycle in addition to a temperature gradient between the legs and arch of the U-bends, promoted accelerated SCC and corrosion damage. As a result, the salt spray test does not accurately indicate SCC susceptibility at these higher temperatures.
- The 43 °C [109 °F] 304 and 304L stainless steels exposed to the salt fog showed evidence of transgranular and intergranular cracking 4 weeks after exposure. Cracking of the 316L stainless steel did not occur until after 32 weeks of exposure. This suggests, as expected, that composition of the alloy plays a role in the SCC susceptibility. However, there are only marginal compositional differences between the 316L and 304 stainless steels. For all alloys, cracking events became more conspicuous as time progressed, and were concentrated within the arch of the U-bends, where pits and general corrosion were also noticeable. Cracking initiated at or near the pits (where residual stresses were also expected to be significant) and propagated through the specimen cross section. Corrosion of the double U-bend specimens was limited to the specimen edges and outer surface and minimal corrosion degradation was observed inside the crevice. This lack of corrosion damage could have resulted from a decrease in salt penetration and deposition inside the crevice. Therefore, the crevices did not appear to preferentially foster corrosion.
- The 85 and 120 °C [185 and 248 °F] 304, 304L, and 316L U-bend specimens exposed to a salt fog showed no SCC formation, consistent with the inability of salt deposited on the specimen surface to deliquesce, even at the high relative humidity values recorded in the chamber. After 32 weeks of exposure, visual observations of the weld specimens exposed to 85 °C [185 °F] indicated the presence of corrosion deposits extending throughout the heat-affected zone in a few specimens. After cleaning, optical examinations showed evidence of a few isolated pits associated with these deposits. The pits appeared to be very superficial and located around the specimen at the heat-affected zone of the weld specimens. The unwelded 85 °C [185 °F] specimens did not exhibit corrosion deposits or pitting. Additionally, none of the specimens held at 120 °C [248 °F] exhibited corrosion deposits or pits throughout the entire exposure time.

- It is speculated that pits in the welded specimens at 85 °C [185 °F] may have developed because of the localized chromium dissolution in the passive layer, which originated weak sites at the metal grain boundary. The dissolution of chromium is typically greater within the heat-affected zone for the weld specimens, especially for the 304 stainless steels, where chromium carbides can precipitate at the grain boundaries during welding. It should be noted that the above mechanism may not be required for SCC or enhanced corrosion of weldments because brittle phase formation in the heat-affected zone can also promote SCC as well as general and localized corrosion.
- The salt fog test is likely conservative because of the high absolute humidity used for the test with respect to the actual conditions observed in a dry storage cask. However, the results are still pertinent because they demonstrate that the deliquescence of dry deposited sea salt can lead to SCC of austenitic stainless steels at temperatures that are only slightly greater than ambient temperatures.
- The estimation of the SCC acceleration factor used in the laboratory testing and its implications on SCC development in actual dry storage cask units in the field are difficult to compute. Under the assumptions presented in this report, the time to SCC initiation is between 32 and 128 weeks for salt deposition geometries that are largely similar to the laboratory testing. This is a rough estimate because it does not take into account the operating history of the dry storage cask and the local environmental conditions at a particular cask location.

7 RECOMMENDATIONS

The results of this investigation indicates that SCC may be observed on austenitic stainless steel canisters used in dry storage systems if certain environmental/material condition combinations are met. To that end, it is important to assess precisely the effect of the service environment on SCC. Understanding the relative humidity and temperature conditions that fall between the deliquescence and efflorescence regions is especially important. This assessment will determine if complete or partial salt deliquescence is required to develop SCC within the service environment.

It is also important to determine salt deposition rates on the stainless steel canisters used in dry storage systems in the field. To accomplish this, it will be necessary to survey environmental conditions around the U.S. to determine critical factors affecting salt precipitation and identify areas of the country more susceptible to atmospheric chloride SCC. One way that this survey can be accomplished is by deploying austenitic stainless steel samples in the field and monitoring SCC development.

In order to more completely evaluate the SCC susceptibility of the stainless steel canisters in actual dry storage systems, a mock-up lab-scale canister prototype containing a heated stressed stainless steel pipe could be used. The mock-up would be instrumented with thermocouples and relative humidity sensors to measure actual conditions inside the dry storage system mock-up. In addition, the mock-up would be instrumented with wetness sensors to determine if salt can deposit and deliquesce at various surface temperatures. The canister mock-up would be exposed to atmospheric conditions obtained from the survey. A computational fluid dynamics modeling would be used to properly scale the mock-up with respect to dry storage system environmental conditions.

8 REFERENCES

ASME. "Rules for Construction of Nuclear Power Plant Components, Division 3, Containment Systems and Transport Packagings for Spent Nuclear Fuel and High Level Radioactive Waste." Section III. ASME Boiler and Pressure Vessel Code. ASTM: New York City, New York. 2003a

ASME. "Welding and Brazing Qualifications." Section IX 2003 Addenda. ASME Boiler and Pressure Vessel Code. ASTM: New York City, New York. 2003b

ASM Handbook: Volume 9: Metallography and Microstructures, G.F. Vander Voort Ed., ASM International. 2004

Assis, J.T., Monin, V., Teodosio, J.R., and Gurova, T. "X-Ray Analysis of Residual Stress Distribution in Weld Region." *Advances in X-Ray Analysis*, Vol. 45. pp. 225-231. 2002

ASTM International. "Standard Practice for Preparation of Stress-Corrosion Specimens for Weldments." ASTM G58-85. West Conshohocken, Pennsylvania: ASTM International. 2005

ASTM International. "Standard Practice for the Preparation of Substitute Ocean Water" ASTM D1141-98. West Conshohocken, Pennsylvania: ASTM International. 2003

ASTM International. "Standard Practice for Making and Using U-Bend Stress Corrosion Test Specimens." ASTM G30-97. West Conshohocken, Pennsylvania: ASTM International. 1997

Cragolino, G.A., Dunn, D.S., Pan, Y.M, and Sridhar, N. "The Critical Potential for the Stress Corrosion Cracking of Fe-Cr-Ni Alloys and Its Mechanistic Implications." *Chemistry and Electrochemistry of Corrosion and Stress Corrosion Cracking: A Symposium Honoring the Contributions of R.W. Staehle*. R.H. Jones, Ed. The Minerals, Metals, and Materials Society, Warrendale, Pennsylvania. 2001

Cui, Y. and Lunding, C.D. "Austenite-preferential Corrosion Attack in 316 Austenitic Stainless Steel Weld Metals." *Mater. Des.* Vol. 28. pp. 324-328. 2007

Fairweather, N.D., Platts, N., and Tice, D.R. "Stress-Corrosion Crack Initiation of Type 304 Stainless Steel in Atmospheric Environments Containing Chloride: Influence of Surface Condition, Relative Humidity, Temperature, and Thermal Sensitization." *Corrosion/2008*, Paper Number 08485, NACE International: Houston, Texas. 2008

Feliu, S., Morcillo. M., and Chico B. "Effect of Distance from Sea on Atmospheric Corrosion Rate." *Corrosion*. Vol. 55. No. 9. pp. 883-891. 1999

Ford, F.P. and Silverman, M.J. "The Prediction of Stress-Corrosion Cracking of Sensitized 304 Stainless-Steel in 0.01 M Na₂SO₄ at 97 °C." *Corrosion*. Vol. 36. pp. 558-565. 1980

- General Motors. "Accelerated Corrosion Test." GM 9540P. Detroit, Michigan: General Motors. 1997
- Goldberg, A. "Comments of the Use of 316L Stainless Steel Cladding at the Geothermal Nilan Test Facility." UCID-17113. Lawrence Livermore Laboratory. Livermore, California. 1976
- Gustafsson, M.E.R. and Franzén, L.G. "Dry Deposition and Concentration of Marine Aerosols in a Coastal Area, SW Sweden." *Atmospheric Environment*. Vol. 30. pp. 977-989. 1996
- Hayes, J.R., Gray, J.J., Szmodis, A.W., and Orme, C.A. "Influence of Chromium and Molybdenum on the Corrosion of Nickel-Based Alloys." *Corrosion*. Vol. 62. pp. 491-500. 2006
- Huizinga, S., J.G. De Jong, W.E. Like, B. McLoughlin, and S.J. Paterson. "Offshore 22Cr Duplex Stainless Steel Cracking - Failure and Prevention." *Corrosion/2009*, Paper Number 05474, NACE International: Houston, Texas. 2005.
- Jorgelius-Pettersen, R.F.A. "Localised Corrosion of Stainless Steels: Ranking, Alloying and Microstructure Effects." *Scand. J. Metall.* Vol. 24. pp. 188-193. 1995
- Larrabee, C.P. "Corrosion Resistance of High Strength Low Alloy Steels as Influenced by Composition and Environment." *Corrosion*. Vol. 9. No. 3. p. 253. 1953
- Leinonen, H. "Stress Corrosion Cracking and Life Prediction Evaluation of Austenitic Stainless Steels in Calcium Chloride Solution." *Corrosion*. Vol. 52. pp. 337-346. 1996
- Lu, B.T., Chen, Z.K., Luo, J.L., Patchett, B.M., and Xu, Z.H. "Pitting and Stress Corrosion Cracking Behavior in Welded Austenitic Stainless Steel." *Electrochimica Acta*. Vol. 50. pp. 1391-1403. 2005
- Macdonald, D.D. "The Point Defect Model for the Passive State." *Journal of the Electrochemical Society*. Vol. 139. pp. 3434-3448. 1992
- Meira, G.R., Andrade, M.C., Padaratz, I.J., Alonso, M.C., and Borba Jr, J.C. "Measurements and Modeling of Marine Salt Transportation and Deposition in a Tropical Region in Brazil." *Atmospheric Environment*. Vol. 40. pp. 5596-5607. 2006
- NASA. "Corrosion Study of Bare and Coated Stainless Steel." MAB 431-68, NASA: Kennedy Space Center, Florida. 1971
- NOAA, "NOAA Satellite and Information Service: National Climatic Data Center." 2009. <<http://www.ncdc.noaa.gov/oa/climate/stationlocator.html>> (5 April 2010)
- Owens, J.S. "Condensation of Water from the Air Upon Hygroscopic Crystals." *Proceedings of the Royal Society of London*. Vol. 110. pp. 738-752. 1926

Prosek, T., Iversen, A., Taxén, C., and Thierry, D. "Low Temperature Stress Corrosion Cracking of Stainless Steels in the Atmosphere in the Presence of Chloride Deposits." *Corrosion*. Vol. 56. pp. 105-117. 2009

Racine, M. "The Effects of Temperature of the Deliquescence of Atmospheric Aerosols." Harvard Undergraduate Research Program. Cambridge, Massachusetts: Harvard University. 2005

Speidel, M.O. "Stress Corrosion Cracking on Stainless Steels in NaCl Solutions." *Metallurgical Transactions*. Vol. 12, pp. 779-789. 1981

Solomon, H.D. *Corrosion*. Vol. 34. No. 6. p. 183. 1978

Sudesh, T.L., Wijesinghe, L., and Blackwood, D.J. "Real Time Pit Initiation Studies on Stainless Steels: The Effect of Sulphide Inclusions." *Corrosion Science*. Vol. 49. pp. 1755-1764. 2007

Szklarska-Smialowska, Z., Xia, Z., and Sharkawy, S.W. "Comparative Studies of SCC in Two Austenitic Stainless Steels and Alloy 600 on Exposure to Lithiated Water at 350 °C." *Corrosion*. Vol. 48. pp. 455-462. 1992

Szklarska-Smialowska, Z. and Gust, J. "The Initiation of Stress Corrosion Cracks and Pits in Austenitic Cr-Ni Steel in MgCl₂ Solutions at 40–90 °C." *Corrosion Science*. Vol. 19. No. 7. pp. 753-766. 1979

Truman, J.E. "The Influence of Chloride Content, pH, and Temperature of the Test Solution on the Occurrence of Stress Corrosion Cracking with Austenitic Stainless Steel." *Corrosion Science*. Vol. 17. pp. 737-746. 1977

Toshima, Y. and Ikeno, Y. "Long-Term Exposure Test for External Stress Corrosion Cracking on Austenitic Stainless Steels in Coastal Areas." *Corrosion/2000*, Paper Number 597, NACE International: Houston, Texas. 2000

Tsai, N.S. and Eagar, T.W. "The Size of the Sensitization Zone in 304 Stainless Steel Welds." *Mat. for Energy Systems*. Vol. 6. No. 1, American Society for Metals. 1984

Tsuruta, T. and Okamoto, S. "Stress Corrosion Cracking of Sensitized Austenitic Stainless Steels in High-Temperature Water." *Corrosion*. Vol. 48. pp. 518-527. 1992

Turnbull, A., Horner, D.A., and Connolly, B.J. "Challenges in Modelling the Evolution of Stress Corrosion Cracks from Pits." *Engineering Fracture Mechanics*. Vol. 76. pp. 633-640. 2009

Tuthill, A.H. "Corrosion Testing of Austenitic Stainless Steel Weldments, *Weld. J.* Vol. 5. pp. 36-40. 2005

Twomey, S. "The Identification of Individual Hygroscopic Particles in the Atmosphere by a Phase-Transition Method." *Journal of Applied Physics*. Vol. 24. pp. 1099-1102. 1953

USNRC. "NAC International Inc., Safety Analysis Report for the UMS Universal Storage System – Docket No. 72-1015." ML003743531, U.S. NRC: Rockville, Maryland. 2003a

USNRC. "Transnuclear Standardized Advanced Nuhoms® Horizontal Modular Storage System for Irradiated Nuclear Fuel Safety Evaluation Report." ML030100468, U.S. NRC: Rockville, Maryland. 2003b

White, W.E. "Observations of the Influence of Microstructure on Corrosion of Welded Conventional and Stainless Steels." Mater. Charact. Vol. 28. pp. 349-358. 1992

Wilde, B.E. "The Role of Passivity in the Mechanism of Stress-Corrosion Cracking and Metal Dissolution of 18Cr-8Ni Stainless Steels in Boiling Magnesium and Lithium Chlorides." Journal of Electrochemical Society. Vol. 118. pp. 1,717-1,725. 1971

Winkler, P. "The Growth of Atmospheric Aerosol Particles with Relative Humidity." Physica Scripta. Vol. 37. pp. 223-230. 1988

Wranglen, G. "Pitting and Sulphide Inclusions in Steel." Corrosion Science. Vol. 14. pp. 331-349. 1974

BIBLIOGRAPHIC DATA SHEET

(See instructions on the reverse)

1. REPORT NUMBER
(Assigned by NRC. Add Vol., Supp., Rev.,
and Addendum Numbers, if any.)

NUREG/CR-7030

2. TITLE AND SUBTITLE

Atmospheric Stress Corrosion Cracking Susceptibility of Welded and Unwelded 304, 304L, and 316L Austenitic Stainless Steels Commonly Used for Dry Cask Storage Containers Exposed to Marine Environments

3. DATE REPORT PUBLISHED

MONTH
October

YEAR
2010

4. FIN OR GRANT NUMBER

N6195

5. AUTHOR(S)

Leonardo Caseres & Todd S. Mintz

6. TYPE OF REPORT

Technical

7. PERIOD COVERED (Inclusive Dates)

8. PERFORMING ORGANIZATION – NAME AND ADDRESS (If NRC, provide Division, Office or Region, U.S. Nuclear Regulatory Commission, and mailing address; if contractor, provide name and mailing address.)

Southwest Research Institute
6220 Culebra Road, P.O. Drawer 28510, San Antonio, Texas 78238-5166

9. SPONSORING ORGANIZATION – NAME AND ADDRESS (If NRC, type "Same as above"; if contractor, provide NRC Division, Office or Region, U.S. Nuclear Regulatory Commission, and mailing address.)

Division of Engineering
Office of Nuclear Regulatory Research
U.S. Nuclear Regulatory Commission
Washington, DC 20555-0001

10. SUPPLEMENTARY NOTES

Mekonen M. Bayssie, NRC Project Manager

11. ABSTRACT (200 words or less)

This report documents information on the susceptibility to atmospheric stress corrosion cracking of welded and unwelded 304, 304L, and 316L austenitic stainless steels commonly used for dry storage containers exposed to marine environments. Standard U-bend specimens were exposed to both salt spray and salt fog conditions at temperatures ranging from 25 to 176 °C [77 to 350 °F] and varying relative humidity. The first test conducted was a salt spray test to scope out material and residual stress effects. This deliberately conservative test resulted in extensive cracking and corrosion as was observed in all the 93 and 176 °C [200 and 350 °F] U-bends in as early as 1 month after exposure. Salt spray tests are non-prototypical since deposition of salt on dry casks is in the form of a dry aerosol; hence, the first test was not suitable for evaluation of stress corrosion cracking susceptibility of austenitic stainless steels in coastal atmospheres. The second test conducted, the salt fog test, was expected to closely simulate field conditions around dry cask containers, and resulted in stress corrosion cracking and pitting corrosion in all the 43 °C [109 °F] specimens. Corrosion developed after 4 weeks in the 304 and 304L specimens, and after 32 weeks in the 316L specimen. This suggests that the alloy composition plays a role in stress corrosion cracking susceptibility. Cracking was mainly transgranular with sections of intergranular branching. Cracks were concentrated within the arch region in all unwelded U-bends and at the heat-affected zone of the welded specimens, as previously reported in the literature. None of the 85 and 120 °C [185 and 248 °F] specimens exposed to the salt fog test exhibited stress corrosion cracking; the data are consistent with the inability of salt deposits to deliquesce at high temperatures.

12. KEY WORDS/DESCRIPTORS (List words or phrases that will assist researchers in locating this report.)

Dry cask
SCC
deliquescence
salt fog
U-bend
austenitic stainless steels

13. AVAILABILITY STATEMENT

Unlimited

14. SECURITY CLASSIFICATION

(This Page)

Unclassified

(This Report)

Unclassified

15. NUMBER OF PAGES

16. ICE PR



Federal Recycling Program

)

)



UNITED STATES
NUCLEAR REGULATORY COMMISSION
WASHINGTON, DC 20555-0001

OFFICIAL BUSINESS